

2016

Candida albicans ISW2 Regulates Chlamyospore Suspensor Cell Formation and Virulence *In Vivo* in a Mouse Model of Disseminated Candidiasis

Dharmika Navarathna

National Cancer Institute, National Institutes of Health, dharmika.h.navarathna.civ@mail.mil

Ruvini U. Pathirana

University of Nebraska-Lincoln

Michail S. Lionakis

National Institute of Allergy and Infectious Diseases, National Institutes of Health

Kenneth W. Nickerson

University of Nebraska-Lincoln, knickerson1@unl.edu

David D. Roberts

National Cancer Institute, National Institutes of Health, droberts@helix.nih.gov

Follow this and additional works at: <http://digitalcommons.unl.edu/bioscifacpub>

 Part of the [Biology Commons](#)

Navarathna, Dharmika; Pathirana, Ruvini U.; Lionakis, Michail S.; Nickerson, Kenneth W.; and Roberts, David D., "*Candida albicans* ISW2 Regulates Chlamyospore Suspensor Cell Formation and Virulence *In Vivo* in a Mouse Model of Disseminated Candidiasis" (2016). *Faculty Publications in the Biological Sciences*. 546.
<http://digitalcommons.unl.edu/bioscifacpub/546>

This Article is brought to you for free and open access by the Papers in the Biological Sciences at DigitalCommons@University of Nebraska - Lincoln. It has been accepted for inclusion in Faculty Publications in the Biological Sciences by an authorized administrator of DigitalCommons@University of Nebraska - Lincoln.

RESEARCH ARTICLE

Candida albicans ISW2 Regulates Chlamyospore Suspensor Cell Formation and Virulence *In Vivo* in a Mouse Model of Disseminated Candidiasis

Dharmika H. M. L. P. Navarathna¹*, Ruvini U. Pathirana²®, Michail S. Lionakis³, Kenneth W. Nickerson², David D. Roberts¹*

1 Laboratory of Pathology, Center for Cancer Research, National Cancer Institute, National Institutes of Health, Bethesda, Maryland, United States of America, **2** School of Biological Sciences, University of Nebraska-Lincoln, Lincoln, Nebraska, United States of America, **3** Fungal Pathogenesis Unit, Laboratory of Clinical Infectious Diseases, National Institute of Allergy and Infectious Diseases, National Institutes of Health, Bethesda, Maryland, United States of America

© These authors contributed equally to this work.

* droboterts@helix.nih.gov (DDR); dharmika.h.navarathna.civ@mail.nih.gov (DHMLPN)



OPEN ACCESS

Citation: Navarathna DHMLP, Pathirana RU, Lionakis MS, Nickerson KW, Roberts DD (2016) *Candida albicans* ISW2 Regulates Chlamyospore Suspensor Cell Formation and Virulence *In Vivo* in a Mouse Model of Disseminated Candidiasis. PLoS ONE 11(10): e0164449. doi:10.1371/journal.pone.0164449

Editor: Martine BASSILANA, Universite de Nice - CNRS, FRANCE

Received: January 20, 2016

Accepted: September 26, 2016

Published: October 11, 2016

Copyright: © 2016 Navarathna et al. This is an open access article distributed under the terms of the [Creative Commons Attribution License](https://creativecommons.org/licenses/by/4.0/), which permits unrestricted use, distribution, and reproduction in any medium, provided the original author and source are credited.

Data Availability Statement: All relevant data are within the paper and its Supporting Information files.

Funding: This study was supported by the Intramural Research Programs of the National Institute of Allergy and Infectious Diseases and the National Cancer Institute, National Institutes of Health (NIH) (M.S.L., AI001175-01; D.D.R., ZIA SC 009173), Ann L. Kelsall and the Farnesol and *Candida albicans* Research Fund, University of Nebraska Foundation (to K.W.N.), and the Blair

Abstract

Formation of chlamyospores by *Candida albicans* was an established medical diagnostic test to confirm candidiasis before the molecular era. However, the functional role and pathological relevance of this *in vitro* morphological transition to pathogenesis *in vivo* remain unclear. We compared the physical properties of *in vitro*-induced chlamyospores with those of large *C. albicans* cells purified by density gradient centrifugation from *Candida*-infected mouse kidneys. The morphological and physical properties of these cells in kidneys of mice infected intravenously with wild type *C. albicans* confirmed that chlamyospores can form in infected kidneys. A previously reported chlamyospore-null $\Delta isw2/\Delta isw2$ mutant was used to investigate its role in virulence and chlamyospore induction. Virulence of the $\Delta isw2/\Delta isw2$ mutant strain was reduced 3.4-fold compared to wild type *C. albicans* or the *ISW2* reconstituted strain. Altered host inflammatory reactions to the null mutant further indicate that *ISW2* is a virulence factor in *C. albicans*. *ISW2* deletion abolished chlamyospore formation within infected mouse kidneys, whereas the reconstituted strain restored chlamyospore formation in kidneys. Under chlamyospore inducing conditions *in vitro*, deletion of *ISW2* significantly delayed chlamyospore formation, and those late induced chlamyospores lacked associated suspensor cells while attaching laterally to hyphae via novel spore-hypha septa. Our findings establish the induction of chlamyospores by *C. albicans* during mouse kidney colonization. Our results indicate that *ISW2* is not strictly required for chlamyospores formation but is necessary for suspensor cell formation. The importance of *ISW2* in chlamyospore morphogenesis and virulence may lead to additional insights into morphological differentiation and pathogenesis of *C. albicans* in the host microenvironment.

Paxton Udale Scholarship for Life Sciences from UNL School of Biological Sciences (to R.U.P.). The funders had no role in study design, data collection and analysis, decision to publish, or preparation of the manuscript.

Competing Interests: The authors have declared that no competing interests exist.

Introduction

Candida albicans is a commensal yeast fungus that is part of the human gastrointestinal and genitourinary tract microbiota. It has emerged as a significant opportunistic pathogen in the growing population of immunocompromised patients, where it causes considerable morbidity, mortality, and health care costs [1–4]. *C. albicans* is now the leading cause of nosocomial bloodstream infection in the USA [5]. Disseminated candidiasis is highly prevalent among immunocompromised cancer patients undergoing chemotherapy [6, 7]. Approximately \$1 billion is spent annually to manage disseminated candidiasis, which has ~40% mortality rate irrespective of treatment with currently available antifungal drugs [8]. The unique morphological plasticity of this pathogen allows *C. albicans* to switch between unicellular yeasts, pseudohyphae, and hyphal forms and contributes to virulence [9]. Under certain environmental conditions, *C. albicans* also differentiates into mating competent opaque cells [10], specifically regulated commensal state GUT (Gastrointestinally Induced Transition) cells [11], and thick-walled chlamydo-spores [12].

Chlamydo-spores, first described in 1877 by Grawitz et al. [13], are the least studied of these morphologic forms and are the only spore type made by *C. albicans*. Chlamydo-spores are large, spherical, thick-walled, and refractile cells that are usually $8\pm 1\ \mu\text{m}$ in diameter, although values from 7 to 12 μm have been reported in the literature. Chlamydo-spores are thought to be formed by rounding off the terminal filamentous hyphae where the basal hyphal compartment has differentiated into a specialized ‘suspensor cell’. Therefore, suspensor cells are considered as a necessary precursor for chlamydo-spore formation in which nuclear division occurs according to the chlamydo-spore developmental model described by Martin et al. [14]. Laboratory conditions that induce chlamydo-spore formation include nutritionally poor media containing complex sugars such as corn meal or rice extract, low temperatures (24–28°C), darkness, and microaerophilic growth under glass cover slips. Chlamydo-spores are non-meiotic, asexual spores. Except for the presence of a thick cell wall, they do not share most common characteristics of classical fungal spores. Their physiological status and role *in vivo* are still uncertain, and they have only been useful for diagnostic differentiation of *C. albicans* and *C. dubliniensis* from other species of *Candida* and other clinically important yeasts [12, 14–22]. So far, little is known about the genetic regulation of chlamydo-spore development in *Candida* species. *C. albicans* *EFG1* is the major transcriptional regulator required for chlamydo-spore formation [20] but it also regulates hyphal transitions. Filamentation is also a prerequisite for chlamydo-spore formation [14]. *NRG1* and *HOG1* signaling are also associated with chlamydo-spore production [15, 23]. A recent study established that the *Candida* cell wall proteins Csp1p and Csp2p are induced specifically in the process of chlamydo-spore production [24].

It is unlikely that chlamydo-spore formation would persist through evolution without a biological function. The presence of *C. albicans* chlamydo-spores *in vivo* during an infection has been reported in a few older clinical case reports [25–27], although these reports were only based on microscopy data. In tissue sections from our previously published animal model studies [28–38], we have consistently observed large spherical cells similar in size to chlamydo-spores which are present in the outer perimeter of *C. albicans* colonies in the mouse kidney cortex (unpublished observations). Our group has remained curious whether these structures are in fact true chlamydo-spores.

Mutant library screening by Nobile et al (2003) found three mutants, $\Delta isw2/\Delta isw2$ (CJN16), $\Delta sch9/\Delta sch9$ (CJN19), and $\Delta suv3/\Delta suv3$ (CJN223) that lacked the ability to induce chlamydo-spores [19]. Based on our preliminary analysis of chlamydo-spore phenotypes in these mutants, $\Delta isw2/\Delta isw2$ was chosen to study the role of *ISW2* (orf19.7401) in chlamydo-spore development and in pathogenesis of disseminated candidiasis. Its closest characterized ortholog, *S. cerevisiae*

Isw2p, is an ATP-dependent chromatin remodeling factor that belongs to the highly conserved ISWI (Imitation Switch) protein family [39–42]. Being an essential factor for protein-DNA interactions on chromatin, *ISW2* also affects the regulation of transcription, recombination, and DNA repair, although the exact mechanisms remain to be elucidated [43]. Moreover, Tsukiyama et al [43] showed that the ISWI gene complexes interact with each other to maintain the chromatin structure, thus allowing survival of yeast cells under stress conditions. Due to the partial localization of Isw2p with microtubules, this protein is also crucial for the expression of early meiotic genes by enabling transcription factors for sporulation specific genes to access chromatin, which in turn initiates sporulation in *S. cerevisiae* [42]. Isw2p also exhibits a repressor activity during mitotic growth of yeast cells following recruitment by Ume6p, a transcription factor involved in both positive and negative regulation of a diverse set of yeast genes [39, 40]. Therefore, *ISW2* may regulate other functions in *C. albicans* in addition to chlamyospore development.

The previously reported *ISW2* null mutant, CJN16, is derived from an avirulent BWP17 parent [19]. Therefore, we constructed an *ISW2* deleted mutant in a prototrophic WT SC5314 *C. albicans* background to investigate the role of this gene in a mouse model of disseminated candidiasis. We report here that deletion of *ISW2* delays the onset of chlamyospore formation without having any discernible defects on cell filamentation or its ability to cope with oxidative stress. Notably, the chlamyospores formed *in vitro* by the $\Delta isw2/\Delta isw2$ mutant are unique in that they form without characteristic suspensor cells and instead form laterally, being attached directly to the hyphae. We report the role of *ISW2* in *in vivo* chlamyospore induction and virulence using a mouse model of disseminated candidiasis. In addition, we confirm previous clinical reports of *in vivo* chlamyospore formation using mouse models.

Materials and Methods

Ethics Statement

Handling and care of mice was conducted in an AAALAC International accredited facility in compliance with the guidelines established by the Animal Care and Use Committee of the National Cancer Institute under approved protocol LP-022. Mice that reached approved humane endpoints were euthanized by CO₂ inhalation.

Strains, media and growth conditions

C. albicans strains SC5314 [44] and A72 (ATCC MYA-2430) [45] were obtained from the American Type Culture Collection, Rockville, MD. *C. dubliniensis* Wü284 strain was kindly provided by Dr. Joachim Morschhäuser from the University of Würzburg, Germany. The strains constructed for this study are listed in Table 1. For routine growth of *C. albicans* strains, YPD medium (10 g/l of yeast extract, 20 g/l of peptone and 20 g/l of glucose with or without 20 g/l of agar) was used. To induce chlamyospore production, *C. albicans* cells grown overnight were plated onto inducing corn meal agar (DIFCO, Detroit, MI or Fluka, Sigma-Aldrich) plates supplemented with 1% Tween 80 according to the Dalmau technique described below. For RNA isolation, corn meal broth medium was prepared by modifying commercially available corn meal agar medium as described previously [46]. Briefly, powdered corn meal agar was suspended in 10% excess of distilled water, continuously stirred overnight at 4°C, and filtered. Staib agar was prepared as described previously [47] using 50 g of *Guizotia abyssinica* plant seed extracted into 1 liter of distilled water and then supplemented with 1 g of glucose, 1 g of KH₂PO₄, 1 g of creatinine, and 15 g of agar.

For mouse infections, *C. albicans* cells were grown overnight in 50 ml of yeast extract-peptone-dextrose (YPD) medium at 30°C aerobically. The *C. albicans* yeast cells were harvested by centrifugation at 4200 × *g* for 10 min, washed twice with 50 ml of sterile nonpyrogenic normal

Table 1. *C. albicans* strains used or constructed in this study.

Strain	Genotype	Reference
SC5314	Wild type (<i>ISW2/ISW2</i>)	[44]
DRL5 ^{NR}	$\Delta isw2::SAT1-FLP/ISW2$	This study
DRL5	$\Delta isw2/ISW2$	This study
DRL6 ^{NR}	$\Delta isw2/\Delta isw2::SAT1-FLP$	This study
DRL6	$\Delta isw2/\Delta isw2$	This study
DRL7 ^{NR}	$\Delta isw2/\Delta isw2::ISW2::SAT1-FLP$	This study
DRL7	$\Delta isw2/\Delta isw2::ISW2$	This study
BWP17	$ura3\Delta::\lambda imm434/ura3\Delta::\lambda imm434 his1::hisG/his1::hisG arg4::hisG/arg4::hisG$	[80]
CJN16	$ura3\Delta::\lambda imm434/ura3\Delta::\lambda imm434 arg4::hisG his1::hisG::pHIS1 isw2::Tn7-UAU1 arg4::hisG his1::hisG isw2::Tn7-URA3$	[19]
CJN19	$ura3\Delta::\lambda imm434/ura3\Delta::\lambda imm434 arg4::hisG his1::hisG::pHIS1 sch9::Tn7-UAU1 arg4::hisG his1::hisG sch9::Tn7-URA3$	[19]
CJN223	$ura3\Delta::\lambda imm434/ura3\Delta::\lambda imm434 arg4::hisG his1::hisG::pHIS1 suv3::Tn7-UAU1 arg4::hisG his1::hisG suv3::Tn7-URA3$	[19]
DAY25	$ura3\Delta::\lambda imm434/ura3\Delta::\lambda imm434 arg4::hisG his1::hisG::pHIS1 rim101::ARG4 arg4::hisG his1::hisG rim101::URA3$	[19]
BH1P1	$BMH1/bmh1\Delta::HIS1 his1\Delta/his1\Delta arg4\Delta::ARG4::URA3/arg4\Delta$	[64]
UdR142C	$bmh1\Delta::HIS1/bmh1\Delta::ARG4 ura3\Delta/ura3\Delta::URA3::bmh1R142C$	[65]

doi:10.1371/journal.pone.0164449.t001

saline, and resuspended in 10 ml of sterile nonpyrogenic saline before cell quantification using a Petroff—Hausser counting chamber. The cell suspensions were adjusted to a final concentration of 1×10^7 cells/ml for parenteral administration using nonpyrogenic sterile saline.

Harvesting and purification of chlamyospores *in vitro*

Radiating *C. albicans* colonies on agar plates were removed using a sterile blade and suspended in 3M sodium thiocyanate in TE buffer. The *C. albicans* laden agar pieces were incubated for 10 min at 50°C with intermittent vortexing to solubilize the agar. After centrifugation at 4,000 rpm for 5 min, the *C. albicans* cell-hypha pellet was resuspended in PBS buffer, and chlamyospores were separated from suspensor cells by sonication (30 s sonication and 30 s resting cycles for 5 min on ice).

Chlamyospores were purified on linear sucrose density gradients [48] of 35–66% w/w (1.15–1.32 g/cc), which were prepared by layering successive 2 ml fractions of decreasing density in 15 ml Beckman polyallomer tubes, whereupon 1–2 ml of sample in 35% sucrose was layered on top. Centrifugation was carried out at 39000 rpm in a SW41 swinging bucket rotor for 12 hours at 10°C in a L70 Beckman ultracentrifuge.

Staining and microscopy of purified chlamyospores

Images of purified chlamyospores, either unstained or stained with Calcofluor White were obtained using light (Olympus, CH3-TR45) and fluorescence (Olympus, BX51TRF) respectively. Images were processed with IPLab software (Scanalytics Inc., Fairfax, VA). For chitin staining, 10% v/v formaldehyde fixed chlamyospores were treated with 0.2 µg/ml Calcofluor White for 5 min in the dark and washed once with xylene. The low concentration of Calcofluor White was chosen to stain chlamyospores predominantly, rather than yeast or hyphae. Size measurements were made with an ocular micrometer and presented as the mean ± standard error of 150 cells.

Construction of $\Delta isw2/\Delta isw2$ mutant and its complementation

To knock out the *ISW2* gene, we followed the *SAT1* flipping strategy reported by Reuss et al, [49] and Sasse & Morschhäuser, [50] using WT *C. albicans* strain SC5314 [44]. The pSFS2A plasmid was kindly provided by Dr. Joachim Morschhäuser from the University of Würzburg, Germany. The unique restriction sites on the left (*ApaI*, *XhoI*) and right (*SacI*, *SacII*) borders of *SAT1* flipper cassette with nourseothricin resistant marker was used for the construction of the *ISW2* gene disruption cassette. The primers used in this study are listed in the Table in S1 File. In brief, the *ApaI-XhoI* fragment of the *C. albicans ISW2* (0.46 kb) upstream flanking sequence was amplified using primer pair, ISW2upleft and ISW2upright. A *SacII-SacI* *ISW2* downstream fragment (0.42 kb) was amplified with primer pair ISW2downleft and ISW2downright. The *ISW2* downstream and upstream fragment was cloned to generate pSFS2A*ISW2down* and then the plasmid with complete gene disruption cassette, pSFS2A*ISW2*, respectively. Transformation for gene knock out was done as we described previously [34, 37] with the *ApaI-SacI* fragment from pSFS2A*ISW2*. The transformants were selected on YPD plates containing 200 µg/ml nourseothricin (JenaBioscience, Germany). The nourseothricin resistance marker in single allele knocked out strain (DRL5^{NR}) was excised by growing in yeast extract-peptone-maltose (YPM) liquid medium as described by Reuss et al. (2004) [49]. This strain, named DRL5, was then transformed again with the same *ApaI-SacI* fragment to make DRL6^{NR} and, following another FLP-mediated excision, generating the *ISW2* homozygous gene knock out mutant, designated as DRL6. The clones were analyzed by sequential Southern hybridization at each step for desired allelic displacement and replacement, using *EcoRI* digested genomic DNA of the transformants with the *ISW2* up and downstream fragments as probes.

The *ISW2* gene complementation cassette was constructed with the *ApaI-XhoI* fragment of the complete *C. albicans ISW2* sequence as well as 0.34 kb of upstream and 0.174 kb of downstream flanking sequences for *ISW2* (3746 bp), amplified using primer pair ISW2compleft and ISW2compright. This fragment was sub-cloned to the *ApaI-XhoI* site in pSFS2A*ISW2down* to generate *ISW2* complementation cassette p*ISW2COMP*. We inserted one copy of the gene back to *ISW2* locus to make the strain $\Delta isw2::ISW2/\Delta isw2$ which was designated as DRL7. Southern hybridization and qRT-PCR analyses confirmed the reintegration of the gene at the correct locus and expression of the reintegrated gene, respectively.

Kinetics of chlamyospore formation *in vitro*

To induce chlamyospore production, log phase cells and cells grown overnight on fresh YPD liquid medium were used as the inoculum because the growth phase was reported to have effects on chlamyospore formation rate [18]. To obtain log phase cells, an overnight YPD liquid culture of *C. albicans* was inoculated into fresh YPD liquid medium at a cell density of ca. 0.01 OD₆₀₀ and incubated for 4–5 hours at 30°C in a 225 rpm rotatory shaker. For each cell type, volumes of 3 µl were used to inoculate either corn meal agar plates supplemented with 1% Tween 80 or Staib agar plates, following the Dalmau technique where cover slips were placed on top of the inoculum to create microaerophilic conditions. The plates were incubated at room temperature in the dark. The plates were examined over the next 6 weeks for *in situ* chlamyospores using an AMG EVOSfl Digital Inverted Microscope.

Filamentous growth and cell cycle growth analysis

The ability to form filaments at 30 or 37°C was determined by incubating *C. albicans* cells in YPD liquid medium as well as under embedded growth conditions. The embedded assay was performed by the pour plate technique with an inoculum of 10⁴ cells/ml in Glucose-Proline-Phosphate (GPP) agar and grown at 37°C for 15 to 17 hours. The ability to form pseudohyphae

was also observed by growing the cells for 4 hours at 37°C in liquid GPP media supplemented with 300 or 600 mM phosphate (1:1 KH_2PO_4 : K_2HPO_4), as described in [51]. All growth patterns were observed *in situ* using AMG EVOSfl Digital Inverted Microscope.

Cell cycle progression was analyzed by nuclear staining with propidium iodide at each time point using a protocol modified from Zhang & Siede [52]. To initiate the cell cycle, G_1 synchronized cells were obtained by a slight modification of a previous protocol [53]. In brief, YPD grown cells were inoculated at 2×10^8 cells/ml into synthetic complete medium without glucose. This carbon deficient liquid medium contained 6.7 g/l of yeast nitrogen base without amino acids (Sigma Y0626), 1.92 g/l of yeast synthetic dropout media without uracil (Sigma Y1501), and 20 mg/l of uracil. Overnight grown cells were inoculated at a final cell density of 2×10^7 cells/ml into fresh YPD liquid medium, grown at 30°C aerobically and then harvested after 0, 1, 2 and 3 hours. The harvested cells were washed once with deionized water, fixed in absolute ethanol for 1 hour, mixed with an aliquot of fresh absolute ethanol, and stored at 4°C until all the samples had been collected. To prepare for flow cytometry, the samples were vortexed extensively, centrifuged for 1 min at $14,000 \times g$, washed with 1 ml of water, and centrifuged again. The cell pellets were resuspended in 1 ml of 50 mM sodium citrate (pH 7.0) and transferred to FACS analysis tubes (BD Falcon 2054) and treated with 8 μl volumes of 10 mg/ml DNase-free RNase A for 1 hour at 50°C. Samples were then incubated with 25 μl of 10 mg/ml proteinase K for another hour. Finally, 1 ml of 20 $\mu\text{g}/\text{ml}$ propidium iodide in 50 mM sodium citrate (pH 7.0) was added in the dark. All samples were briefly sonicated just before analysis on a BD FACSCanto™ II with FACSDiva version 6.1.1 software. Actual cell numbers were statistically analyzed using ANOVA on GraphPad Prism software.

Mouse infection with *C. albicans*

Outbred 6–8 week old (18–20 g) BALB/c female mice obtained from the NCI Frederick mouse breeding facility were randomly allocated to groups of five animals and housed and cared with *ad libitum* access to filtered water and standard mouse chow. For the survival study, WT (SC5314), DRL6 ($\Delta isw2/\Delta isw2$), and DRL7 ($\Delta isw2::ISW2/\Delta isw2$) strains were inoculated into three groups of 15 mice with a control group getting only sterile non pyrogenic saline. Each group was inoculated intravenously in the lateral caudal tail vein using a 27 gauge needle with a volume of 0.1 ml containing 10^6 *C. albicans* cells of each respective strain [28, 30, 31]. Clinical signs of illness in each mouse were evaluated three times daily, and mice that displayed humane endpoints including arched back posture, sunken eyes, ruffled hair, or dehydration were euthanized immediately by CO_2 inhalation and processed for complete necropsy and collection of tissues for histopathological examination. To examine basic host immune responses, two groups of mice were infected with the WT SC5314 and DRL6 strains, and euthanized at 2 days post-inoculation (PI) for organs and sera collection. Five mice were inoculated with the WT SC5314, five were inoculated with DRL6 strain, and five control mice received 0.1 ml saline i.v with no fungal challenge. Sera separated from the blood collected from individual mice were stored at -80°C until analysis. Kidneys of infected mice consisting of 5 mice per group infected with WT SC5314, DRL6, or DRL7 strains were stored at -80°C for subsequent use to extract total RNA for analysis of chlamyospore-specific gene expression at day 3 post-infection.

Necropsy and histopathology

Immediately after euthanasia, macroscopic changes were recorded, and the brain, heart, lungs, liver, spleen, and right kidneys were immersed in buffered 10% formalin, processed for paraffin embedding, sectioned at 5 μm , and stained with haematoxylin and eosin (H&E). Grocott's modification of Gomori's methenamine-silver (GMS) stain was used for detection of fungi *in*

situ [35, 37]. Histopathology images from sections of formalin-fixed and paraffin-embedded tissues stained with GMS or H&E were obtained using a light microscope (Olympus BX51) fitted with a digital camera (Nikon DXM1200F) and ScanScope XT digital scanner (Aperio). Images were processed with Adobe Photoshop and Aperio ImageScope v11.1.2.760 (Aperio).

Determination of serum cytokines and chemokines

Murine serum was collected from sacrificed mice at 2 days PI following infection with *C. albicans* WT and mutant strains. A Luminex-bead array (Mouse cytokine/Chemokine Milliplex MAP Kit, catalog no MPXMCYTO-70K, Millipore, Billerica, MA) was used to detect the cytokines IL-6, IL-10 IL-17, TNF- α , IL-1 β , GM-CSF and chemokines MCP1, MIP1- α and RANTES according to the manufacturer's specifications.

Statistical analysis

The probability of survival as a function of time was determined by the Kaplan-Meier method, and significance was determined by the log-rank (Mantel-Cox) test and Jehan-Breslow-Wilcoxon test using GraphPad Prism software. Serum cytokine expression patterns among all treatment groups at 2 days PI were analyzed by two-way ANOVA with the post Bonferroni comparison test. Three to four randomly selected mice from each group were euthanized at each time point for longitudinal comparisons. Data were analyzed for significant differences by comparing means of each triplicate reading at various time points assuming that the cytokine expression levels within each group of mice were normally distributed.

Expression of chlamyospore specific markers *in vitro* and *in vivo*

For *in vivo* gene expression analysis, total RNA was extracted from kidneys infected with *C. albicans* WT, DLR6, and DLR7 strains. *In vitro* gene expression analysis was performed in the same strains grown in corn meal broth and YPD broth at different time points up to 5 days using a phenol extraction method as described [54], and the absence of genomic DNA was confirmed by a forward PCR primer within the *ACT1* intron (P26) and a reverse primer within the distal exon (PN90) as described previously [55] and/or DNase treatment using TURBO DNA-free™ Kit (Invitrogen). One hundred ng of total RNA were used to prepare first strand cDNA using SuperScript® III First-Strand Synthesis SuperMix for qRT-PCR (Invitrogen™) according to the manufacturer's recommendation using oligo(dT) primers. Quantitative PCR was conducted using iQ™ SYBR® Green Supermix in a Biorad CFX Connect® real-time PCR detection system. Each cDNA preparation was normalized using *CaCDC36* as an internal control. The primers used in this study are listed in the Table in S1 File. Quantitative RT-PCR data were normalized in two steps as described previously [34] and analyzed using two-way ANOVA with the post Bonferroni comparison test.

Results

Chlamyospore-like structures in mouse kidneys infected with *C. albicans*

Kidneys are the primary colonization organ in the mouse model of disseminated candidiasis [30, 31, 56, 57]. The mouse immune system can clear the initial *C. albicans* infection from other organs, so the outcome of the infection depends on how fungal colonization progresses in the kidneys [58]. Yeast cells escape from nephrons and settle in peri-glomerular regions of the kidney as early as 2 to 6 hours PI [34]. Initially, the yeast cells grow as micro-colonies composed of mixtures of yeasts and filaments, which subsequently overwhelm the kidney cortex as

early as 2 days PI [30, 34]. The host response consists of strong monocyte/macrophage and neutrophil infiltration together with high levels of TNF- α and IL-6 and other pro-inflammatory cytokines, which creates a local inflammatory response, leading to tissue injury and necrosis, kidney malfunction, and the formation of granulation tissues around the *C. albicans* colonies starting at 3 to 7 days PI [34, 37]. At this stage we observed large spherical cells ca. 6–8 μm in size in histopathological sections stained with GMS (Fig 1). These spherical cells were limited in number and were mainly visualized in the periphery of the resolving lesions caused by extensive fungal colonization (Fig 1, middle panel). We frequently observed these large spherical cells in the kidney cortexes of mice from day 3 PI onwards (Fig 1), and we have observed them in most of our previous studies [28–38] with both WT *C. albicans* A72 and SC5314 in the mouse model for disseminated candidiasis (unpublished observations).

In vitro and *in vivo* characterization of chlamydo spores

We isolated these large cells using isopycnic sucrose density gradient centrifugation. Chlamydospore morphology was confirmed by Calcofluor White staining after purification. On 35 to 66% (w/w) linear gradients yeasts, hyphae, and pseudohyphae banded at ca. 1.28–1.29 g/cc, whereas the chlamydo spores banded at ca. 1.17 g/cc (Fig 2, top panel). This lower density for chlamydo spores is consistent with the presence of refractile lipid granules as observed by phase contrast microscopy as well as the high lipid content ($\geq 20\%$) reported by Jansons and Nickerson [59] and the sucrose flotation purification described for chlamydo spores by Fabry et al [17]. Without sonication the chlamydo spores remained attached to hyphae and banded at an intermediate density of ca. 1.22–1.24 g/cc. Chlamydo spores produced *in vitro* on cornmeal agar were identical with those formed *in vivo* three days PI in mouse kidneys with regard to their banding position on sucrose density gradients (Fig 2). Purified *in vitro* chlamydo spores and thin histological sections of *Candida* infected kidneys were stained with Calcofluor White and observed by fluorescence microscopy (Fig 2A and 2B), while *in vitro* and *in vivo* purified unstained chlamydo spores were examined by phase contrast microscopy at 1000X (Fig 2C and 2D). When compared with the *in vitro* cells, *Candida* infected kidney sections stained using Calcofluor White showed cells with the expected size of chlamydo spores (Fig 2B). Critically, the *in vitro* and *in vivo* chlamydo spores banded at the same density (1.17 g/cc, Fig 2, top panel) and had the same diameter ($8.0 \pm 1 \mu\text{m}$, Fig 2C and 2D). These properties indicate that the chlamydo spore-like structures observed in kidney sections in the mouse model of disseminated candidiasis are indeed chlamydo spores.

Chlamydo spore mutant phenotypes in a BWP17 background

We reexamined the chlamydo spore null mutants $\Delta isw2/\Delta isw2$ (CJN16), $\Delta sch9/\Delta sch9$ (CJN19) and $\Delta suv3/\Delta suv3$ (CJN223) originally identified by Nobile et al [19]. The mutants were grown under microaerophilic conditions on corn meal agar for four weeks, and WT SC5314 and BWP17 strains were included for comparison. During the first three weeks, in agreement with previous findings [19], none of the mutants produced chlamydo spores. However, prolonged incubation up to four weeks showed some chlamydo spores in both $\Delta sch9/\Delta sch9$ and $\Delta suv3/\Delta suv3$ mutants, which structurally resembled the chlamydo spores formed by WT SC5314 (Fig 3A versus 3B & 3C). More interestingly, the $\Delta isw2/\Delta isw2$ (CJN16) mutant also showed late induction of chlamydo spores during the fifth week with the unusual feature that the $\Delta isw2/\Delta isw2$ mutant chlamydo spores were located laterally, attached directly to the hyphae, and apparently without the usual suspensor cells (Fig 3D). For this reason, we chose to study further the function of *ISW2* in a virulent background.

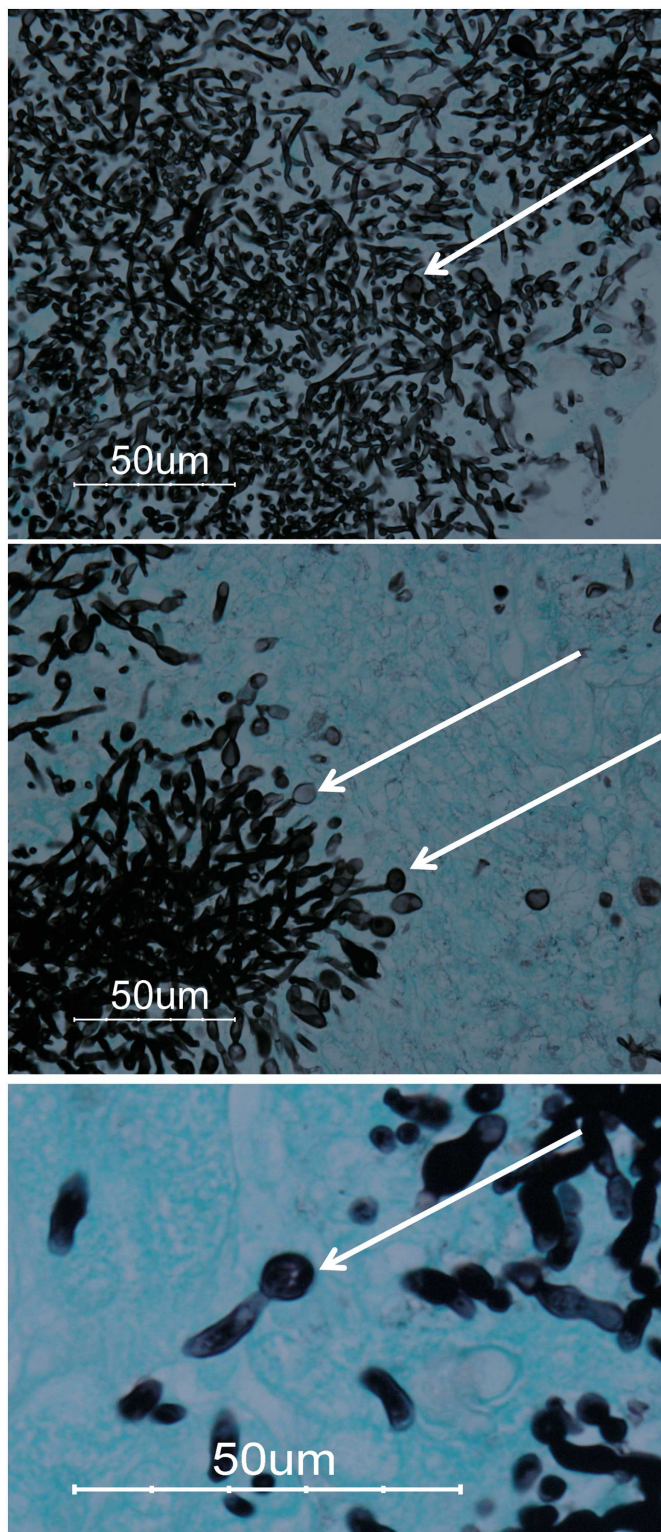


Fig 1. Chlamydospore-like structures are observed in *C. albicans*-infected mouse kidneys at day 3 post-inoculation. Top panel: A representative section from infected kidney cortex stained using GMS three days PI with *C. albicans*. Chlamydospore-like structures are indicated by the arrows. Middle panel: Periphery of a resolving *Candida*-infected lesion shows isolated chlamydospore-like structures (arrows). Bottom panel: Higher magnification of the same histopathology sections shows spherical fungal spores with a diameter of 8 μm .

doi:10.1371/journal.pone.0164449.g001

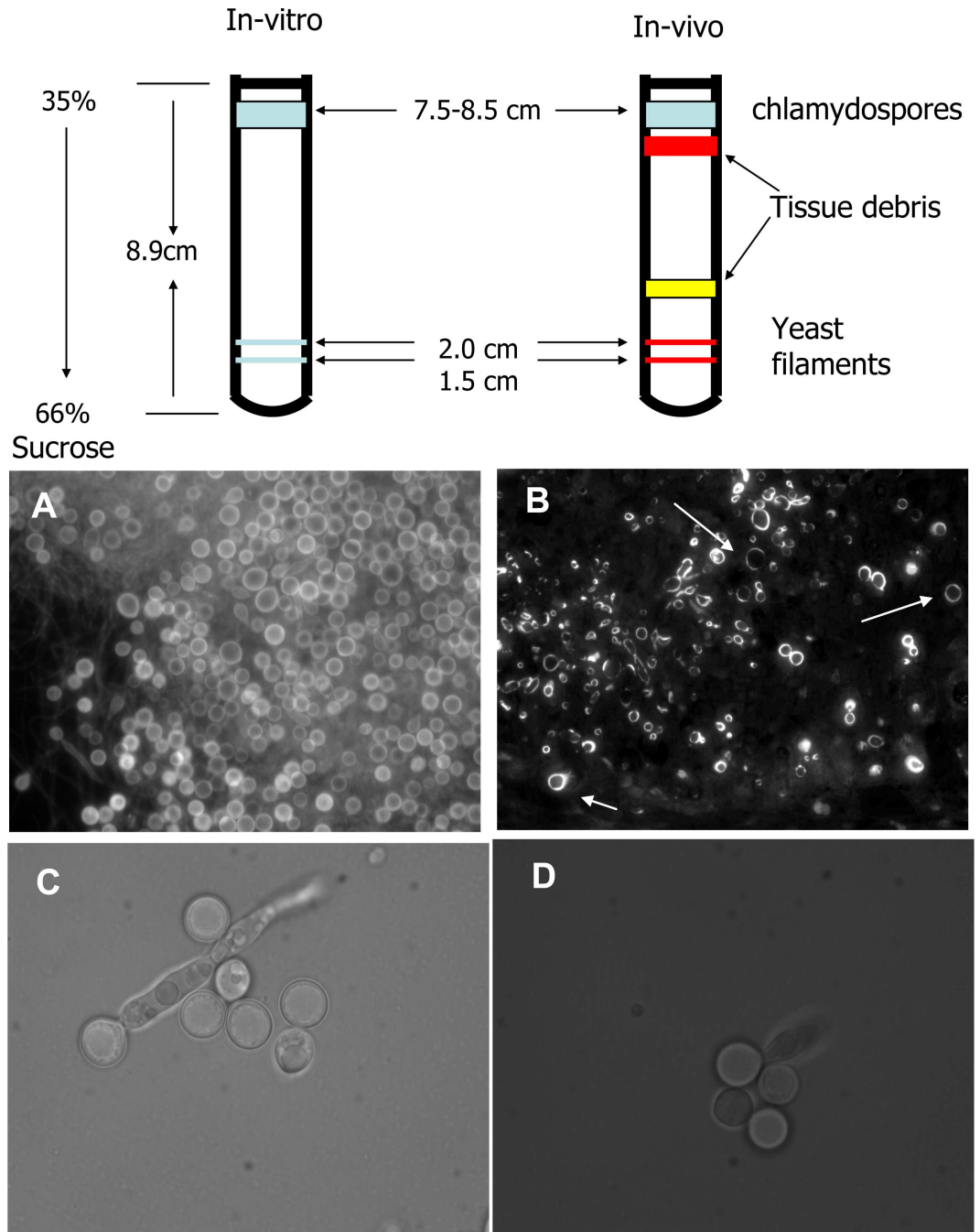


Fig 2. Purification of chlamydospores by sucrose density gradient. Top panel: Schematic diagram showing sedimentation pattern for chlamydospores, yeast, and filamentous *C. albicans* after ultracentrifugation on a sucrose density gradient. Bottom panel: A. Gradient purified chlamydospores from *in vitro* cultures imaged under fluorescence microscopy after staining with Calcofluor White. B. Thin section of infected mouse kidney 3 days PI with *C. albicans* and stained with Calcofluor White (*in vivo*). C & D Unstained chlamydospores examined under phase contrast microscopy at 1000X (C, *in vitro*; D, *in vivo*). A and C, purified chlamydospores from *C. albicans* A72 grown in cornmeal agar; B and D, harvested from *C. albicans* A72 infected kidneys 102 h PI.

doi:10.1371/journal.pone.0164449.g002

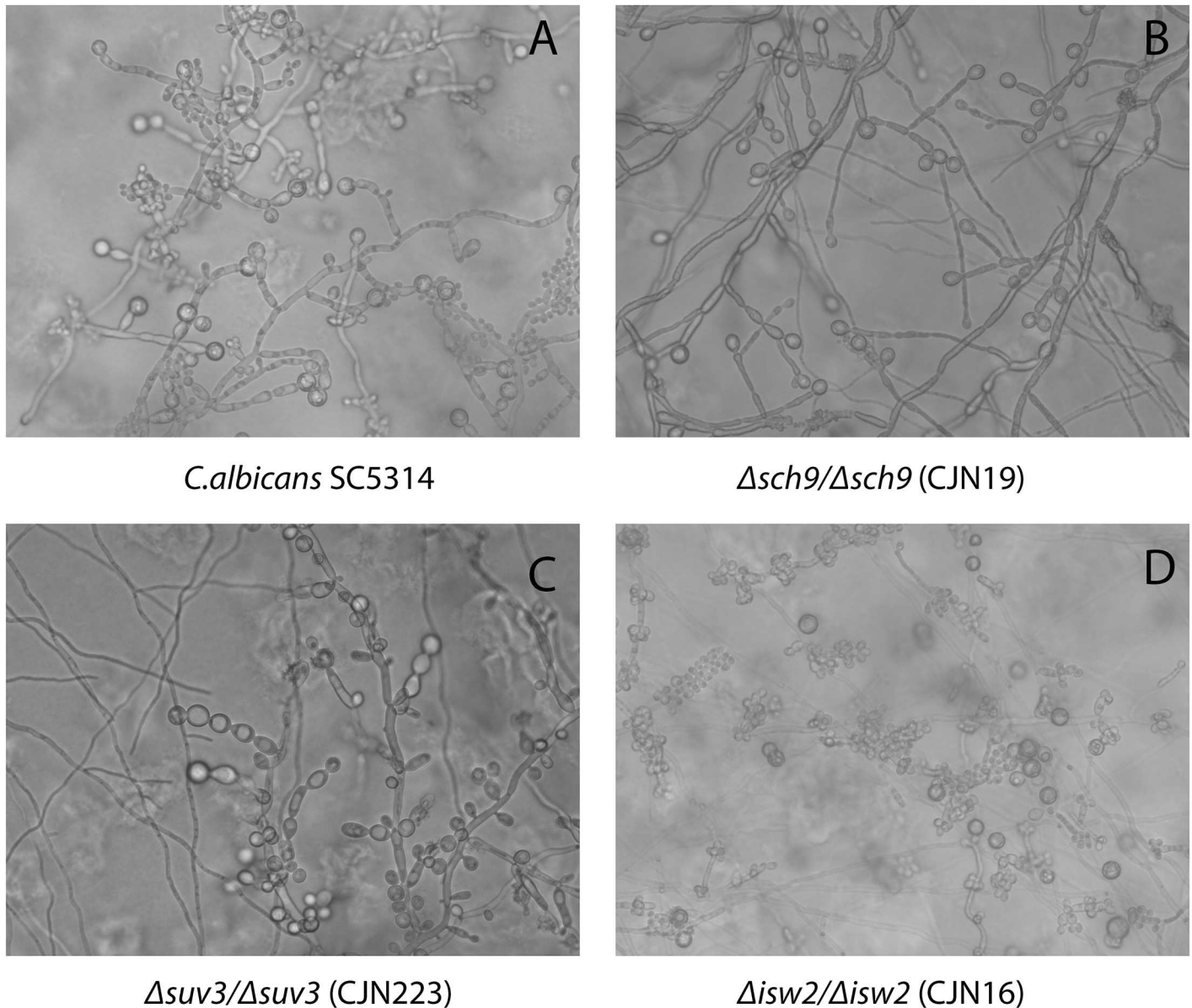


Fig 3. Morphology and timing of chlamydospore formation in WT *C. albicans* and CJN19, CJN223 and CJN16 strains grown on corn meal agar. (A) *C. albicans* SC5314 (10 days); (B) *C. albicans* CJN19 ($\Delta sch9/\Delta sch9$, 25 days) (C) *C. albicans* CJN223 ($\Delta suv3/\Delta suv3$, 25 days) and (D) *C. albicans* CJN16 ($\Delta isw2/\Delta isw2$, 35 days). Imaging was performed *in situ* in corn meal agar plates under bright field using an AMG EVOSfl Digital Inverted Microscope.

doi:10.1371/journal.pone.0164449.g003

ISW2 deletion altered *in vitro* chlamydospore formation

The chlamydospore-null mutants described by Nobile et al are insertion mutants derived from auxotrophic strain BWP17 (*ura3::imm434/ura3::imm434 iro1/iro1::imm434 his1::hisG/his1::hisG arg4/arg4*) [19]. Some *URA3* blasted gene deletion strains are avirulent in mouse models due to positional effects on expression of reintroduced *URA3* or the unintended deletion of *IRO1*, a virulence factor tightly linked to *URA3* gene [60–63]. To avoid such potential artifacts in subsequent mouse virulence studies, we constructed a $\Delta isw2/\Delta isw2$ mutant in a prototrophic background using the method of Reuss et al. [49, 50] as we previously reported [30, 34].

Consistent with the report by Nobile et al [19], our *ISW2* deleted (DRL6) strain constructed in the fully virulent SC5314 WT background did not exhibit chlamyospore production up to 21 days following induction (Fig 4A), while the reconstituted strain formed mature chlamyospores within 14 days (Fig 4A). However, during the fourth week of incubation, the DRL6 strain formed laterally located, chlamyospore-like thick walled cells, connected to the hyphae without any intervening suspensor cells (Fig 4A and 4B). These putative chlamyospores were harvested and purified by sucrose density gradients, where they banded at the same low density as WT chlamyospores, a feature characteristic of their high lipid content [59]. Microscopy of these putative chlamyospores revealed thick-walled spheres with diameters of $7.9 \pm 1 \mu\text{m}$ as expected for chlamyospores. Furthermore, the cells were readily stained with low concentrations of Calcofluor White (Fig 4B), which revealed that the lateral chlamyospores made by DRL6 were directly connected to the hyphae by spore-hypha septa (Fig 4B). These septa are important because they indicate a regulated sporulation process rather than merely a cytoplasmic burst through a weakened cell wall.

Notably, we have also observed the rare appearance of chlamyospores lacking suspensor cells in aged WT SC5314 cultures (Fig 4A). We also compared several previously described mutants with abnormal chlamyospore phenotypes [19, 64, 65] for longer incubation periods to verify that suspensor cells are specifically regulated by *ISW2* gene. Among those chlamyospore-defective mutants, DAY25 (*rim101Δ/rim101Δ*) [19], hyphal growth defective BH1P1 (*BMH1/bmh1Δ*), and UdR142C (*bmh1Δ/bmh1Δ*) [64, 65] showed a similar abundance of chlamyospore formation as the WT strains with sporadic occurrence of chlamyospores without suspensor cells by the end of five weeks of incubation. Due to the presence of chlamyospores, with and without suspensor cells and their small numbers with the latter phenotype, these observations are not comparable to that of *ISW2* deletion strains of DRL6 or CJN19. Therefore, *ISW2* may play a regulatory role in formation of suspensor cells for the chlamyospores and the onset of chlamyospore formation.

Effect of *ISW2* deletion on filamentation, cell cycle progression, and stress responses

Based on previous observations that filamentation is a prerequisite for chlamyospore formation [14], we examined the filamentous growth capabilities of the DRL6 strain under two standard filament inducing conditions (YPD liquid and GPP embedded agar, both at 37°C) and found no differences compared with WT *C. albicans* (Fig 5A–5C). Furthermore, the DRL6 strain readily formed hyphae on corn meal agar that were indistinguishable from WT hyphae.

We examined cell cycle progression profiles of the DRL6 strain compared to its WT parent. Propidium iodide-stained cells were examined via flow cytometry and by quantification of the cell numbers (Fig 5D). No differences in cell cycle phase distribution (G1 vs. G2) were observed between DRL6 and SC5314 strains under the standard growth conditions.

C. albicans confronts diverse stresses during host adaptation and pathogenicity. Because many genes identified in chlamyospore formation are also involved in stress responses [15, 19], we carried out spot dilution assays to examine the stress tolerance of the DRL6 strain towards H₂O₂ (up to 4.0 mM), sodium chloride (up to 1.5 M), sorbitol (up to 2.0 M), and farnesol (up to 200 μM). None of these stress inducers differentially affected the growth rate of DRL6 versus WT SC5314 strains at the concentrations tested (data not shown). This absence of hypersensitivity to oxidative stress is consistent with previous observations for the CJN16 strain [19]. Taken together, the absence of defects in filamentation, cell cycle progression, and stress responses in DRL6 mutant makes it more likely that *ISW2* has a specific function in the timing of chlamyospore formation via the presence or absence of suspensor cells.

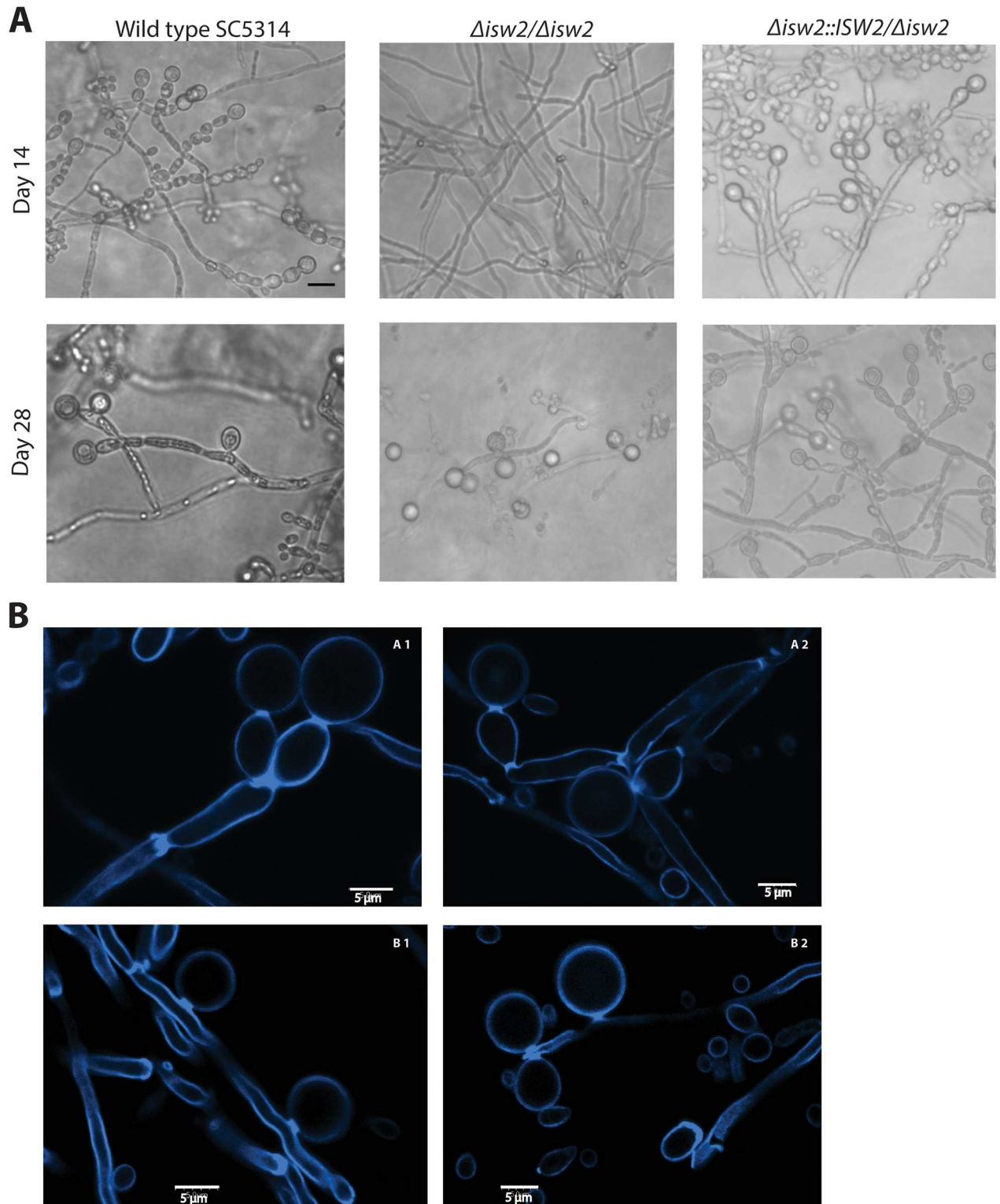


Fig 4. Late induction of chlamydospores lacking suspensor cells in $\Delta isw2/\Delta isw2$ mutant strain compared to its parent strain. (A) Time course of chlamydospore development over six weeks to verify a developmental pattern of chlamydospores lacking suspensor cells in DRL6 ($\Delta isw2/\Delta isw2$) strain. Images captured at 2 and 4 weeks are shown. The WT SC5314 and *ISW2* complemented DRL7 strains initiated chlamydospore formation within 5 to 10 days on corn meal agar supplemented with 1% Tween 80. In contrast, the DRL6 ($\Delta isw2/\Delta isw2$) strain had no visible chlamydospores by day 14 but did produce lateral chlamydospores without suspensor cells after 4 to

5 weeks of incubation. **(B)** Micrographs of Calcofluor White-stained chlamyospores from *C. albicans* SC5314 (A1, A2) and the DRL6 ($\Delta isw2/\Delta isw2$) strain (B1, B2) captured after 2 and 4 weeks of incubation, respectively, with an Olympus FV500 Inverted (Olympus IX-81) Confocal Microscope. The average size of the WT chlamyospores formed on suspensor cells are 8.32 ± 0.94 (SD) μm , whereas the chlamyospores lacking suspensor cells are 7.88 ± 1.12 (SD) μm ; $n = 50$. The images were analyzed with ImageJ (NIH) software for diameter measurement.

doi:10.1371/journal.pone.0164449.g004

ISW2 deletion promotes chlamyospore formation in Staib agar

Chlamyospore formation in Staib agar is diagnostic for *C. dubliniensis* in that *C. albicans* is unable to induce chlamyospores in the same medium [47]. Later, Staib and Morschhäuser showed that down regulation of *NRG1* in *C. dubliniensis* allows chlamyospore formation in Staib agar and, as a corollary, that *CaNRG1* acts as a repressor of this ability. Consequently, the *nrg1Δ/nrg1Δ* mutant of *C. albicans* produced chlamyospores in Staib medium [21, 23]. In *C. albicans*, the *NRG1* gene encodes a transcriptional repressor of filamentation that acts in part synergistically with *TUP1* gene, a transcriptional corepressor. Therefore, we examined the growth behavior of DRL6 ($\Delta isw2/\Delta isw2$) strain on Staib agar in comparison to *C. dubliniensis* and WT SC5314. Within a week of incubation, *C. dubliniensis* produced filaments and

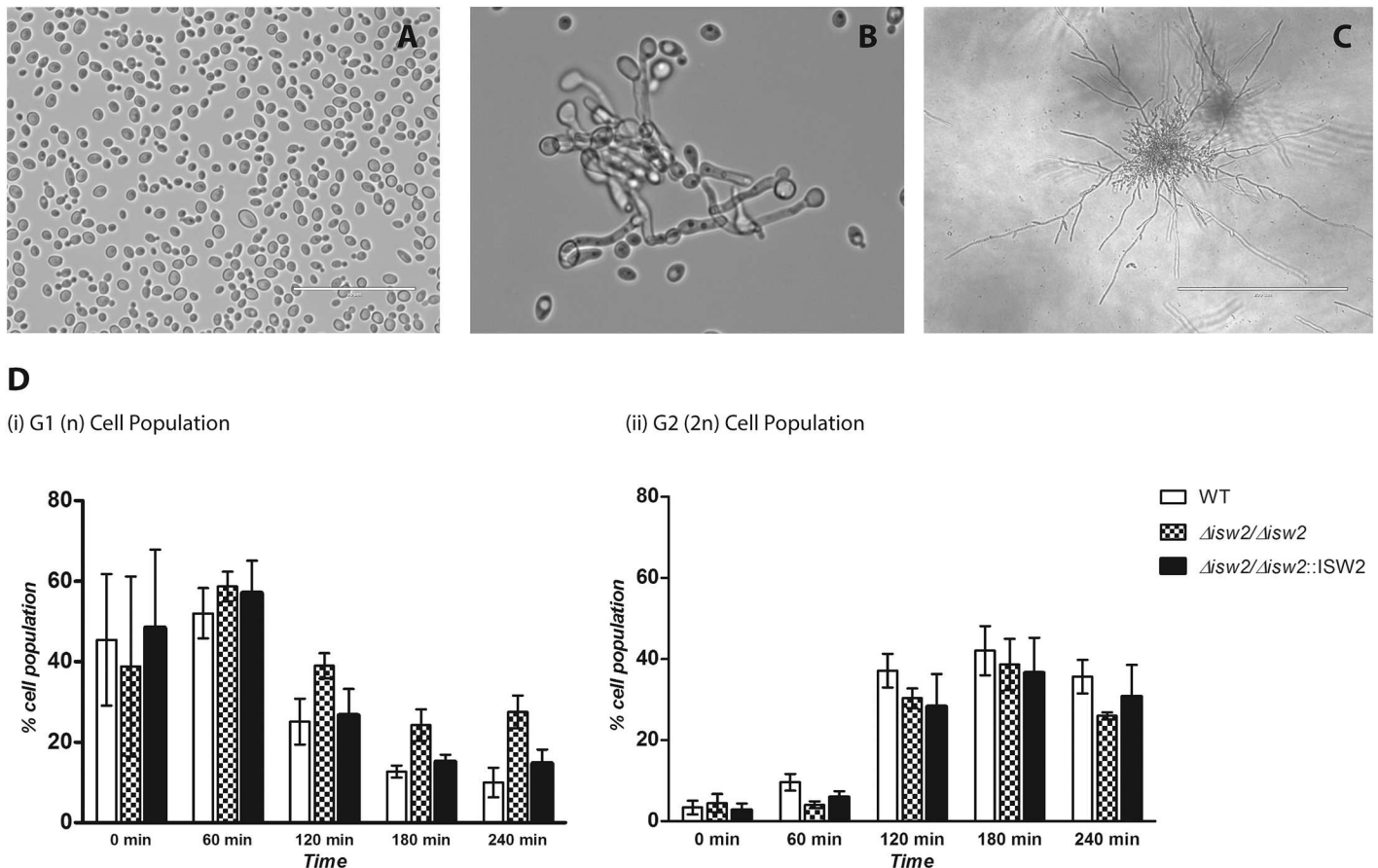


Fig 5. Filamentation morphologies and cell cycle progression is unaltered by ISW2 deletion. **(A)** Yeast cell morphology after overnight growth in YPD at 30°C. **(B)** Hyphal formation after overnight growth in YPD at 37°C. **(C)** Vigorous filamentation in embedded GPP agar after 16 hrs at 37°C. **(D)** Histograms from flow cytometry analysis of cell cycle for each cell population (G1 and G2) percentage from three biological replicates. Representative flow cytometry plots shows that cell cycle progression is similar to that of WT strain. G1 synchronized cells were analyzed via a time course with PI staining as described under Materials and Methods.

doi:10.1371/journal.pone.0164449.g005

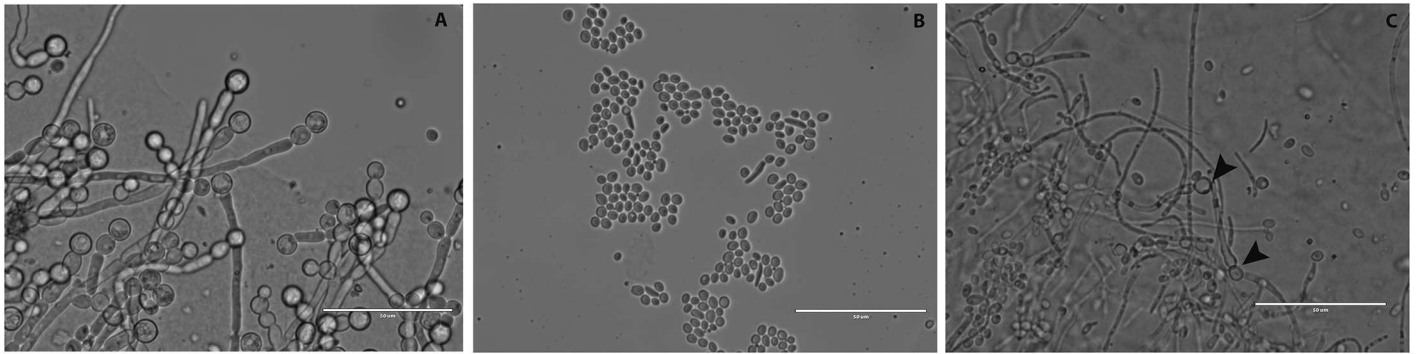


Fig 6. DRL6 induces chlamyospores in Staib agar. (A) Abundant chlamyospore formation by *C. dubliniensis* Wü284. (B) Poor filamentation and no detectable chlamyospores by *C. albicans* SC5314. (C) Occasionally visible chlamyospore formation by DRL6 ($\Delta isw2/\Delta isw2$) strain in Staib agar as indicated by the black arrow heads. Plates were grown at room temperature in the dark for up to 7 days, and representative pictures are from at least 3 independent experiments.

doi:10.1371/journal.pone.0164449.g006

chlamyospores (Fig 6A) whereas SC5314 as expected, failed to produce filaments or chlamyospores (Fig 6B). Surprisingly, the DRL6 strain showed moderate filamentation and sporadic occurrence of some conventional prototype chlamyospores (i.e. with suspensor cells) on Staib agar (Fig 6C). We have never observed chlamyospores with suspensor cells for the DRL6 strain on corn meal agar. The $\Delta nrg1/\Delta nrg1$ mutant was reported to produce chlamyospores occasionally on corn meal agar [23]. Thus, the appearance of chlamyospores with suspensor cells on Staib agar is intriguing because it shows that suspensor cell production is nutritionally regulated.

ISW2 deletion reduces virulence and alters the inflammatory immune response in the mouse model of disseminated candidiasis

The well-established mouse model of disseminated candidiasis was used to compare virulence among the WT, DRL6 ($\Delta isw2/\Delta isw2$), and DRL7 ($\Delta isw2::ISW2/\Delta isw2$) strains. Mice infected with the DRL6 strain had a significantly higher survival rate compared with mice infected with the WT SC5314 strain ($n = 15$, $p < 0.001$, Fig 7A). A control group of mice that received sterile non-pyrogenic saline i.v. did not show any mortality. The Gehan-Breslow-Wilcoxon test hazard ratio estimates indicated 3.4-times greater lethality for WT infection compared to infection by the DRL6 strain. Complementation of one allele in the DRL7 strain restored virulence to the level of the WT parent strain and significantly increased virulence compared with the DRL6 strain (Fig 7A, $p < 0.001$).

We screened a panel of cytokines and chemokines at day 2 PI to assess the innate immune response to infection. WT infected mice had significantly higher serum levels of IL-6, TNF- α , IL-10 and MIP1- α compared with both the mutant infected mice and the uninfected control group (Fig 7B). Deletion of ISW2 did not significantly alter the responses to infection of serum cytokines IL-17, IL-1 β , GM-CSF and the chemokines MCP-1 and RANTES relative to that observed in infected WT mice (Figure A in S1 File).

Absence of chlamyospores in kidneys infected with the DRL6 mutant

We next examined the *in vivo* formation of chlamyospores by the DRL6 strain compared to WT SC5314. We examined infected mouse kidneys harvested from the survival assays (Fig 7A) described in the previous section to determine whether DRL6 strain lost its ability to form chlamyospore-like structures *in vivo*. Infected kidneys were examined at the subacute phase (day

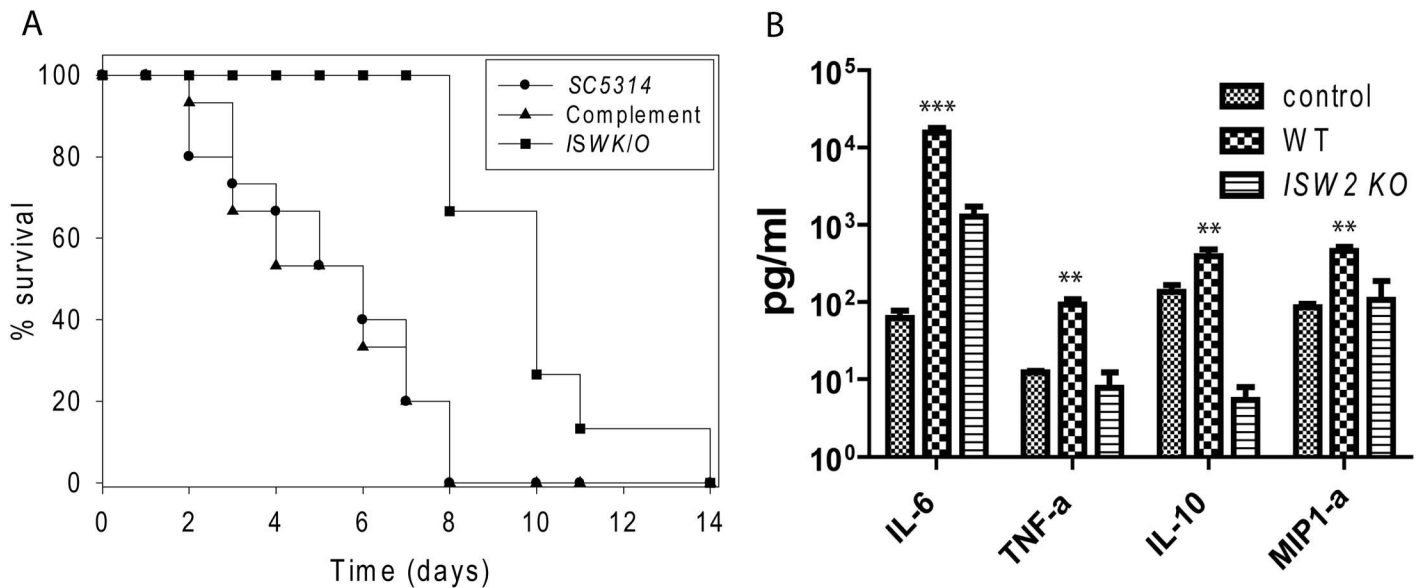


Fig 7. Deletion of *ISW2* prolongs survival in the mouse model of systemic candidiasis and alters host cytokine and chemokine expression. (A) Effect of *ISW2* deletion on mouse survival following intravenous *C. albicans* injection. Survival of mice injected with WT *C. albicans* SC5314 (●), the null mutant DRL6 ($\Delta isw2/\Delta isw2$) (■) and single copy reconstituted DRL7 (▲). Gehan-Breslow-Wilcoxon test hazard ratio estimates indicated 3.4-times greater lethality for WT infection compared to infection by the DRL6 strain. (n = 15; p<0.001, uninfected control = 6, data not shown). (B) Effects of *ISW2* expression in *C. albicans* on host serum cytokine and chemokine induction after infection. Serum levels of the indicated cytokines (IL-6, TNF- α , IL-10, and MIP1 α) were assessed at day 2 PI for mice infected with WT (checkerboard) or DRL6 ($\Delta isw2/\Delta isw2$) strain (horizontal lines) and statistically compared with both uninfected control and mutant. Control (crosshatch) values at day 0 are mean values determined for sera from five uninfected mice. Quantitative data represent mean \pm SEMD. ** = p< 0.01; *** = p< 0.001.

doi:10.1371/journal.pone.0164449.g007

3–6) when the kidney cortex is predominantly colonized and chlamyospore-like structures are first observed [34]. Thorough examination of representative sections showed no chlamyospore-like structures in kidneys from mice infected using the DRL6 strain (Figure B in S1 File). In contrast, we consistently observed chlamyospore-like cells in kidneys from mice infected with SC5314 or the *ISW2*-complemented DRL7 strains (Fig 8). Therefore, the large cells (arrow heads) noted in GMS stained sections from WT and DRL7 strains are most likely chlamyospores, as indicated by the 100 μ m size bar positioned at the bottom of the panel (Fig 8). A few solitary chlamyospores, indicated by the arrow in a representative section at day 8 PI, were visible in SC5314 WT infected kidney matrix in the resolution phase. Furthermore, we did not observe overwhelming kidney colonization by DRL6 compared with the characteristic phenotypes of SC5314 and DRL7 strains (Figure B in S1 File), consistent with the lower virulence of the DRL6 strain (Fig 7A). Otherwise, the DRL6 strain did not deviate from the kidney pathogenesis pattern of WT [30, 34, 35] and progressed to medullary colonization at the chronic stage of kidney infection (Figure B in S1 File).

CSP1 and *CSP2* gene expression *in vivo* and *in vitro*

We investigated expression of two recently reported chlamyospore-associated markers, *CSP1* (orf19.3512) and *CSP2* (orf19.4170) [24], *in vivo* in infected kidneys at day 3 PI (Fig 9). We examined *ISW2*, *CSP1* and *CSP2* gene expression in DRL6 and DRL7 strain infected kidneys compared with SC5314 WT infected kidneys. Three days coincides with the onset of mortality for WT *C. albicans* (Fig 7A) and our current and previous observations of chlamyospore appearance in infected kidneys. Interestingly, neither *CSP1* nor *CSP2* expression was affected by *ISW2* deletion (p < 0.05) under these *in vivo* conditions (Fig 9).

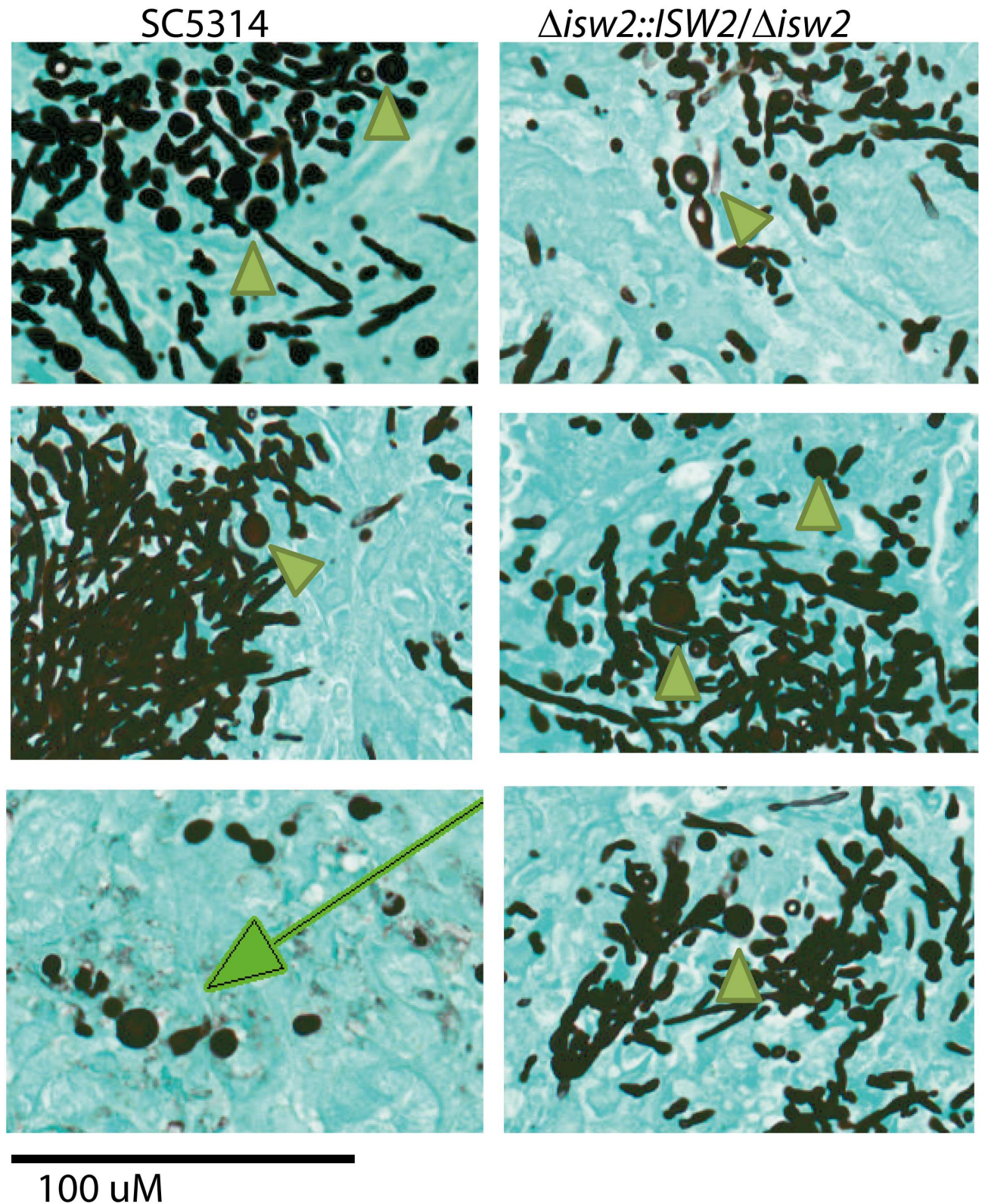


Fig 8. *Isw2p* expression induces chlamyospore formation in kidneys of mice with disseminated candidiasis. Representative GMS stains of kidney sections dissected from mice infected with WT, and reconstituted DRL7 strains. Arrowheads indicate representative chlamyospores in histological sections of infected mouse kidneys at 3–6 days PI. Large arrow in left-lower corner image indicates a solitary chlamyospore in a resolving lesion in mouse kidney cortex at 8 days PI. Scale bar, 100 μ m.

doi:10.1371/journal.pone.0164449.g008

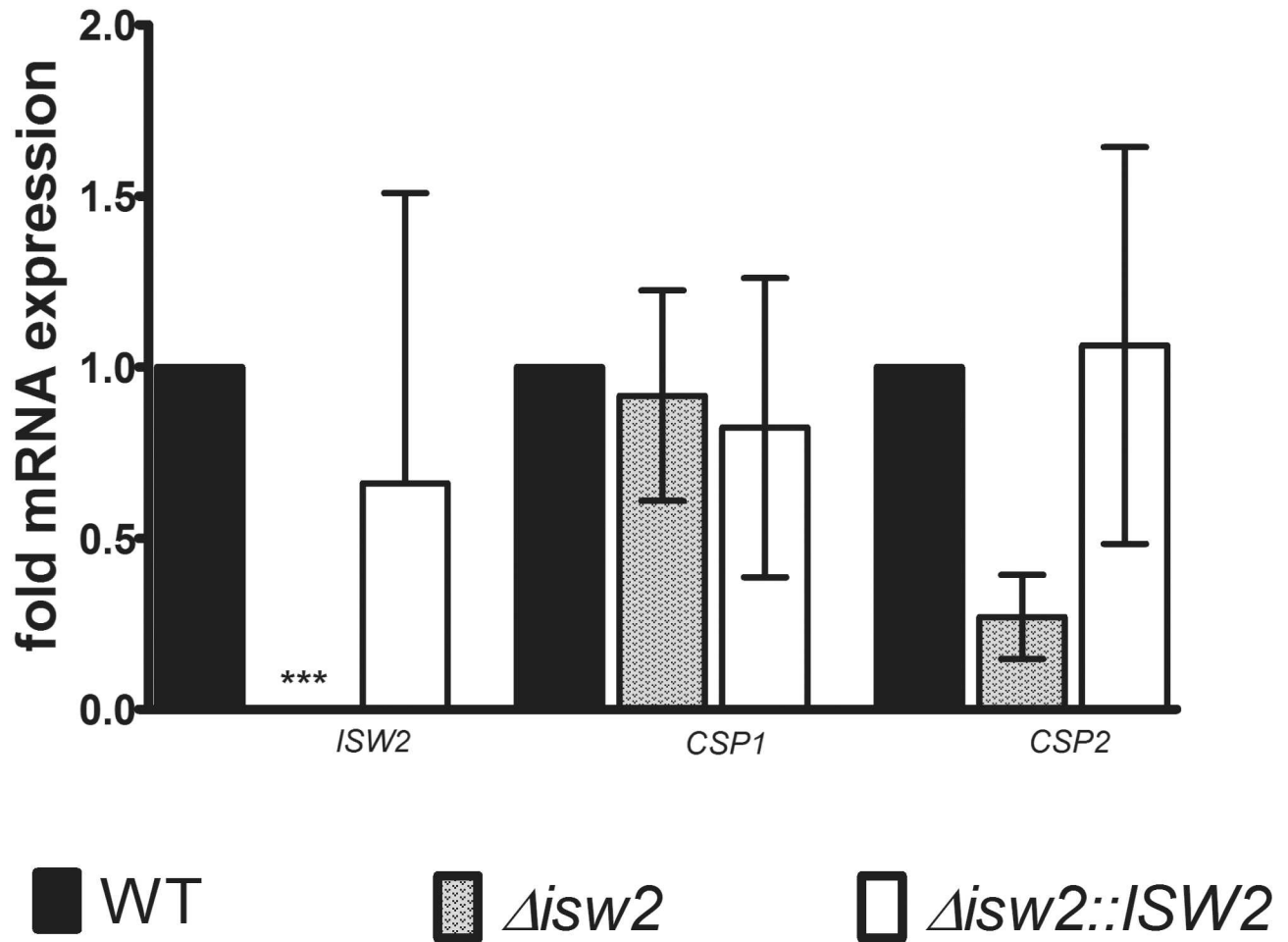


Fig 9. Expression of the chlamyospore-specific genes *CSP1* and *CSP2* during *in vivo* growth of *C. albicans*. qRT-PCR analysis of total RNA extracted from infected mouse kidneys harvested at 3 days PI showing that *CSP1* and *CSP2* were expressed during infection *in vivo* by all three strains. Expression is presented normalized to 1 for the WT strain, where mean Ct values were 24.3 for *ISW2*, 35.59 for *CSP1*, and 35.61 for *CSP2*. Results represent mean \pm SD from three biological replicates. *** = $p < 0.001$.

doi:10.1371/journal.pone.0164449.g009

In parallel, we compared the expression of *CSP1* and *CSP2* in cells grown in YPD and corn meal broth. Basal expression of *CSP1* in YPD was not significantly affected by deletion of *ISW2*, whereas *CSP2* expression decreased in the mutant and was restored in the complemented strain (Figure C panel B in [S1 File](#)). Growth of the *ISW2* deletion mutant in cornmeal medium for five days in the dark resulted in significant induction of *CSP2* mRNA relative to that in YPD or basal expression in corn meal medium (Figure C panel D, F in [S1 File](#)). In the same strain, *CSP1* showed significant induction relative to basal expression in cornmeal medium on day 5 but not relative to that in YPD (Figure C panel C, E in [S1 File](#)). No significant changes in *CSP1* or *CSP2* expression were observed in corn meal medium for WT SC5314 or the reconstituted strain. These data suggest that *ISW2* is not necessary for induction of *CSP1* or *CSP2* expression. The previously reported strong upregulation of *CSP1* and *CSP2* during chlamyospore induction may depend on undefined factors in Staib or rice extract media that are not optimal in corn meal medium.

Discussion

In vivo chlamyospore formation during *C. albicans* infections and their role in virulence have been poorly studied to date. Here we document the formation of chlamyospores in *Candida*-infected mouse kidneys and reduced virulence of a $\Delta isw2/\Delta isw2$ strain in a mouse model of disseminated candidiasis that coincides with an absence of chlamyospores in infected kidneys. We also identify *ISW2* as a gene that is not required for chlamyospore formation but rather determines the timing and morphology of chlamyospore development. In an *ISW2* null background, chlamyospores form laterally from the hyphae without an apparent suspensor cell, which challenges the dogma that suspensor cells are necessary for chlamyospore formation. Although the *ISW2* deleted strain is defective in producing suspensor cells, *ISW2* is not necessary for filamentation, cell cycle progression, or induction of the chlamyospore markers *CSP1* and *CSP2* in corn meal medium. Delayed chlamyospore induction upon *ISW2* deletion under laboratory conditions is consistent with the absence of chlamyospores in kidneys infected with this strain at day 3 PI.

The ability to produce chlamyospores *in vitro* under inducing conditions is nearly universal among clinical isolates of *C. albicans* [66]. Given that yeast-mycelia morphogenesis is fundamental to the dissemination and virulence of *C. albicans*, we reasoned that chlamyospore morphogenesis may also play some pathophysiological role. Defining a role of chlamyospores in *C. albicans* pathogenesis requires careful analysis of clinical samples to exclude chlamyospores associated with secondary mycotic infections. Chlamyospores resemble large blastococidia of *C. albicans* [67, 68] and a variety of morphological forms of the common fungal pathogens *Cryptococcus neoformans*, *Blastomyces dermatitidis*, and *Paracoccidioides brasiliensis* [67]. Such confusion in diagnosis could be prevented by identifying unique morphological, physiological and molecular features of *C. albicans* chlamyospores. Their characteristically large size compared to vegetative cells, staining characteristics including their double walled spherical morphology, distinctive buoyant density, the presence of lipid granules, gene expression, and association with suspensor cells confirm the chlamyospore formation by *C. albicans in vitro* as well as *in vivo*.

Chlamyospore-like structures were previously reported in human clinical specimens from skin, brain, gastrointestinal tract, endocardium and kidneys [26, 69–71]. A clinical case report noted giant forms of *C. albicans* that resemble chlamyospores in multiple organs including the lungs and pancreas [67]. Those authors suggested that treatment with antimicrobial agents could have induced formation of these large structures. Chlamyospore-like structures were also observed in the gastrointestinal tract of infected immunocompromised mice [25]. Candidiasis patients were found to produce antibodies reactive with chlamyospores [72].

Most of these early reports of *in vivo* chlamyospores predate the identification of *C. dubliniensis* in 1995 as a new *Candida* species that forms chlamyospores more readily than does *C. albicans* [73]. Therefore, these early clinical observations cannot be attributed to *C. albicans* rather than *C. dubliniensis*. We have also observed variation within *C. albicans* in that strains A72 and 10231 form chlamyospores more readily and abundantly than SC5314 (unpublished observation).

The expression of *CSP1* and *CSP2* in the DRL6 ($\Delta isw2/\Delta isw2$) mutant *in vitro* and in infected kidneys is consistent with a RNASeq analysis of a *C. albicans* $\Delta nrg1$ mutant or *C. dubliniensis* grown in Staib medium, which did not find significant changes in *ISW2* or other genes important for chlamyospore formation including *SUV3*, and *SCH9* relative to WT *C. albicans* [19, 24]. Therefore, *ISW2* expression is not dependent on *CSP1* or *CSP2* expression levels under the specific growth conditions studied. Conversely, deletion of *ISW2* decreased the basal expression of *CSP2* mRNA in YPD but did not alter transient induction of *CSP1* or *CSP2*

gene expression in cornmeal medium. Although Csp1p and Csp2p protein expression is specific for chlamyospores, the mRNAs encoding these proteins are also expressed basally in YPD medium where no chlamyospores are present [24], and we have confirmed this result in our strains. Therefore, regulation of Csp1p and Csp2p protein levels may occur post-transcriptionally, and background expression of their mRNAs by yeast cells precludes any conclusion that the CSP1 or CSP2 mRNA expression we observed in infected kidneys is associated with chlamyospores.

The reduced virulence of the *ISW2* null mutant DRL6 in a mouse model of disseminated candidiasis was associated at day 2 PI with decreased up-regulation of IL-6, TNF- α , MIP1- α , and IL-10, cytokines and chemokines that are known to play a role in innate host defense against *Candida in vivo* [58, 74, 75]. These differences may simply reflect the lower fungal load associated with the mutant *Candida* strain, but further investigation into the effects of *ISW2* on the host immune response is warranted. The persistence of chlamyospores we observed in resolving *Candida* lesions in infected mouse kidney cortex suggests a potential role in resistance to host immunity.

C. albicans ISW2 is not well-studied, but potential functions can be predicted based on studies of the *S. cerevisiae* ortholog. A BLAST (bl2seq) search of the amino acid sequence of Isw2p of *C. albicans* (orf19.7401) versus Isw2p of *S. cerevisiae* (YOR304W) using the NCBI BLASTP tool identified 61% identity and 77% similarity between the two sequences. The yeast replicative life span was extended robustly upon *ISW2* deletion in *S. cerevisiae*, which was accompanied by derepression of a cohort of stress responses genes [76]. This negative regulation mechanism was also observed in *C. elegans* as well as in other complex eukaryotes [41, 76], providing further evidence for a highly conserved function of the ISWI subfamily. However, we did not observe enhanced sensitivity to osmotic or oxidative stress in the DRL6 strain compared with the WT SC5314 parent, and therefore delayed chlamyospore formation could not be solely attributed to differential stress responses in the mutant strain [76]. The question remains whether suspensor cell and/or chlamyospore formation could be governed by a nutritional stress rather than an oxidative or osmotic stress.

The mechanism by which the *ISW2* deletion induces regular chlamyospores in Staib agar needs further investigation because *C. albicans* does not induce chlamyospores in Staib agar except with a $\Delta nrg1/\Delta nrg1$ mutant. One possibility is downregulation of *NRG1* in the *ISW2* deleted DRL6 strain. *In vitro* chlamyospore formation is typically induced in unusual growth media with complex carbohydrate sources. Nutrient depletion conditions can signal stress responses via the TOR signaling pathway and the *ISW2*-regulated pathway [76]. *SCH9* encodes a nutrient-responsive protein kinase that acts in parallel to TOR to regulate replicative life span [77]. *C. albicans* $\Delta sch9/\Delta sch9$ (CJN19) also exhibits defects in its chlamyospore formation kinetics (This study and [19]). Since chlamyospore formation occurs upon prolonged incubation, which results in accumulation of aged cells, and is limited to nutritionally-poor media such as corn meal agar or rice extract agar, such caloric restriction conditions may regulate unknown chlamyospore-inducing genes.

Our studies identify *ISW2* as a regulator of the *C. albicans* suspensor cells associated with chlamyospore formation. Our finding of chlamyospore formation in the absence of suspensor cells could account for the previously reported lateral chlamyospores in WT isolates [78]. Further physical and molecular characterization is needed to confirm those morphological observations. Preliminary morphological evidence for direct formation of chlamyospores from yeast cells has also been reported [79]. However, the infrequent occurrence of lateral chlamyospores in aged yeast cultures needs further examination. Many details of the molecular function of Isw2p in *C. albicans* remain unclear. Identifying infection-associated genes regulated by Isw2p will be paramount to understanding the developmental and regulatory steps

governing chlamydospore formation and their contribution to pathogenesis and modulation of host responses during systemic and mucosal *C. albicans* infections.

Supporting Information

S1 File. Table. Primers used in this study. Underlined segment indicate the custom restriction sites inserted for constructing pSFS2A*ISW2* and p*ISW2COMP*. **Figure A. Host serum cytokine and chemokine responses after infection show no significant dependence on ISW2.** The cytokines IL-17, IL-1 β , GM-CSF as well as the chemokines MCP-1, and RANTES did not exhibit significant differences at day 2 PI for mice infected with WT (checkerboard) or DRL6 (Δ *isw2*/ Δ *isw2*) strain (horizontal lines). Control (crosshatch) values at day 0 are mean values determined for sera from five uninfected mice. Quantitative data represent mean \pm SEM. **Figure B. Histopathological observations in kidney sections of mice infected with WT, DRL6 (Δ *isw2*/ Δ *isw2*) mutant and reconstituted DRL7 strains.** Representative GMS stains of kidney sections dissected from mice infected with *ISW2* deleted DRL6, showing no chlamydo-spores in comparison to the wild type and *ISW2* complemented strain where arrowheads indicate representative chlamydo-spores. **Figure C. Expression of the chlamydo-spore-specific genes *CSP1* and *CSP2* during *in vitro* growth of *C. albicans*.** *C. albicans* SC5314, DRL6, and DRL7 strains were grown *in vitro* in corn meal or YPD broth media, and total RNA was isolated at days 1, 2, 3 and 5. Basal expression in YPD is shown in panels A and B. The fold expression of *CSP1* and *CSP2* in cornmeal medium were normalized to respective gene expression on day 1 under non-inducing (C, D) and inducing conditions respectively (E, F). qRT-PCR analysis showed that *ISW2* deletion significantly affected the expression of the chlamydo-spore-specific markers, *CSP1* (A) and *CSP2* only on day 5 (B). Results represent mean \pm SD from three biological replicates. Quantitative data represent mean \pm SD. * = $p < 0.05$; ** = $p < 0.01$; *** = $p < 0.001$.

(PDF)

Acknowledgments

We thank Dr. Joachim Morschhäuser for providing plasmids and strains and Dr. Aaron Mitchell and Dr. Joy Sturtevant for providing mutant strains. We thank Dr. Wayne Riekhof for providing AMG EVOSfl Digital Inverted Microscope facility and Dr. Steve Harris for helpful discussion.

Author Contributions

Conceptualization: DHMLPN RUP KWN DDR.

Data curation: KWN DDR.

Formal analysis: DHMLPN RUP.

Funding acquisition: KWN MSL DDR.

Investigation: DHMLPN RUP MSL.

Methodology: DHMLPN RUP KWN DDR.

Project administration: KWN DDR.

Resources: KWN DDR.

Supervision: KWN DDR.

Validation: DHMLPN RUP MSL.

Visualization: DHMLPN RUP.

Writing – original draft: DHMLPN RUP MSL KWN DDR.

Writing – review & editing: DHMLPN RUP MSL KWN DDR.

References

1. Diekema D, Arbefeville S, Boyken L, Kroeger J, Pfaller M. The changing epidemiology of healthcare-associated candidemia over three decades. *Diagn Microbiol Infect Dis*. 2012; 73:45–48. doi: [10.1016/j.diagmicrobio.2012.02.001](https://doi.org/10.1016/j.diagmicrobio.2012.02.001) PMID: [22578938](https://pubmed.ncbi.nlm.nih.gov/22578938/)
2. Labelle AJ, Micek ST, Roubinian N, Kollef MH. Treatment-related risk factors for hospital mortality in *Candida* bloodstream infections. *Crit Care Med*. 2008; 36:2967–2972. doi: [10.1097/CCM.0b013e31818b3477](https://doi.org/10.1097/CCM.0b013e31818b3477) PMID: [18824910](https://pubmed.ncbi.nlm.nih.gov/18824910/)
3. Pfaller MA, Jones RN, Messer SA, Edmond MB, Wenzel RP. National surveillance of nosocomial blood stream infection due to species of *Candida* other than *Candida albicans*: frequency of occurrence and antifungal susceptibility in the SCOPE Program. SCOPE Participant Group. Surveillance and Control of Pathogens of Epidemiologic. *Diagn Microbiol Infect Dis*. 1998; 30:121–129. PMID: [9554180](https://pubmed.ncbi.nlm.nih.gov/9554180/)
4. Pfaller MA, Moet GJ, Messer SA, Jones RN, Castanheira M. *Candida* bloodstream infections: comparison of species distributions and antifungal resistance patterns in community-onset and nosocomial isolates in the SENTRY Antimicrobial Surveillance Program, 2008–2009. *Antimicrob Agents Chemother*. 2011; 55:561–566. doi: [10.1128/aac.01079-10](https://doi.org/10.1128/aac.01079-10) PMID: [21115790](https://pubmed.ncbi.nlm.nih.gov/21115790/)
5. Magill SS, Edwards JR, Bamberg W, Beldavs ZG, Dumyati G, Kainer MA, et al. Multistate point-prevalence survey of health care-associated infections. *N Engl J Med*. 2014; 370:1198–1208. doi: [10.1056/NEJMoa1306801](https://doi.org/10.1056/NEJMoa1306801) PMID: [24670166](https://pubmed.ncbi.nlm.nih.gov/24670166/)
6. Slavin MA, Sorrell TC, Marriott D, Thursky KA, Nguyen Q, Ellis DH, et al. Candidaemia in adult cancer patients: risks for fluconazole-resistant isolates and death. *J Antimicrob Chemother*. 2010; 65:1042–1051. doi: [10.1093/jac/dkq053](https://doi.org/10.1093/jac/dkq053) PMID: [20202987](https://pubmed.ncbi.nlm.nih.gov/20202987/)
7. Sipsas NV, Lewis RE, Tarrand J, Hachem R, Rolston KV, Raad II, et al. Candidemia in patients with hematologic malignancies in the era of new antifungal agents (2001–2007). *Cancer*. 2009; 115:4745–4752. doi: [10.1002/cncr.24507](https://doi.org/10.1002/cncr.24507) PMID: [19634156](https://pubmed.ncbi.nlm.nih.gov/19634156/)
8. Trick WE, Fridkin SK, Edwards JR, Hajjeh RA, Gaynes RP. Secular trend of hospital-acquired candidemia among intensive care unit patients in the United States during 1989–1999. *Clin Infect Dis*. 2002; 35:627–630. doi: [10.1086/342300](https://doi.org/10.1086/342300) PMID: [12173140](https://pubmed.ncbi.nlm.nih.gov/12173140/)
9. Gow NA, van de Veerdonk FL, Brown AJ, Netea MG. *Candida albicans* morphogenesis and host defence: discriminating invasion from colonization. *Nat Rev Microbiol*. 2012; 10:112–122. doi: [10.1038/nrmicro2711](https://doi.org/10.1038/nrmicro2711) PMID: [22158429](https://pubmed.ncbi.nlm.nih.gov/22158429/)
10. Miller MG, Johnson AD. White-opaque switching in *Candida albicans* is controlled by mating-type locus homeodomain proteins and allows efficient mating. *Cell*. 2002; 110:293–302. doi: [10.1016/S0092-8674\(02\)00837-1](https://doi.org/10.1016/S0092-8674(02)00837-1) PMID: [12176317](https://pubmed.ncbi.nlm.nih.gov/12176317/)
11. Pande K, Chen C, Noble SM. Passage through the mammalian gut triggers a phenotypic switch that promotes *Candida albicans* commensalism. *Nat Genet*. 2013; 45:1088–1091. doi: [10.1038/ng.2710](https://doi.org/10.1038/ng.2710) PMID: [23892606](https://pubmed.ncbi.nlm.nih.gov/23892606/)
12. Staib P, Morschhauser J. Chlamyospore formation in *Candida albicans* and *Candida dubliniensis*—an enigmatic developmental programme. *Mycoses*. 2007; 50:1–12. doi: [10.1111/j.1439-0507.2006.01308.x](https://doi.org/10.1111/j.1439-0507.2006.01308.x) PMID: [17302741](https://pubmed.ncbi.nlm.nih.gov/17302741/)
13. Grawitz P. Zur Botanik des Soors und der Dermatomyosen. *Dtsch Z Prakt Med*. 1877; 20:209–211.
14. Martin SW, Douglas LM, Konopka JB. Cell cycle dynamics and quorum sensing in *Candida albicans* chlamyospores are distinct from budding and hyphal growth. *Eukaryot Cell*. 2005; 4:1191–1202. doi: [10.1128/ec.4.7.1191-1202.2005](https://doi.org/10.1128/ec.4.7.1191-1202.2005) PMID: [16002645](https://pubmed.ncbi.nlm.nih.gov/16002645/)
15. Alonso-Monge R, Navarro-García F, Román E, Negredo AI, Eisman B, Nombela C, et al. The Hog1 mitogen-activated protein kinase is essential in the oxidative stress response and chlamyospore formation in *Candida albicans*. *Eukaryotic Cell*. 2003; 2:351–361. PMID: [12684384](https://pubmed.ncbi.nlm.nih.gov/12684384/)
16. Citiulo F, Moran GP, Coleman DC, Sullivan DJ. Purification and germination of *Candida albicans* and *Candida dubliniensis* chlamyospores cultured in liquid media. *FEMS Yeast Res*. 2009; 9:1051–1060. doi: [10.1111/j.1567-1364.2009.00533.x](https://doi.org/10.1111/j.1567-1364.2009.00533.x) PMID: [19538507](https://pubmed.ncbi.nlm.nih.gov/19538507/)

17. Fabry W, Schmid EN, Schrapf M, Ansorg R. Isolation and purification of chlamyospores of *Candida albicans*. *Med Mycol*. 2003; 41:53–58. PMID: [12627804](#)
18. Jansons VK, Nickerson WJ. Induction, morphogenesis, and germination of the chlamyospore of *Candida albicans*. *J Bacteriol*. 1970; 104:910–921. PMID: [4099098](#)
19. Nobile CJ, Bruno VM, Richard ML, Davis DA, Mitchell AP. Genetic control of chlamyospore formation in *Candida albicans*. *Microbiology*. 2003; 149:3629–3637. doi: [10.1099/mic.0.26640-0](#) PMID: [14663094](#)
20. Sonneborn A, Bockmuhl DP, Ernst JF. Chlamyospore formation in *Candida albicans* requires the Efg1p morphogenetic regulator. *Infect Immun*. 1999; 67:5514–5517. PMID: [10496941](#)
21. Staib P, Morschhauser J. Liquid growth conditions for abundant chlamyospore formation in *Candida dubliniensis*. *Mycoses*. 2005; 48:50–54. doi: [10.1111/j.1439-0507.2004.01085.x](#) PMID: [15679667](#)
22. Vidotto V, Bruatto M, Accattatis G, Caramello S. Observation on the nucleic acids in the chlamyospores of *Candida albicans*. *New Microbiol*. 1996; 19:327–334. PMID: [8914134](#)
23. Staib P, Morschhäuser J. Differential expression of the NRG1 repressor controls species-specific regulation of chlamyospore development in *Candida albicans* and *Candida dubliniensis*. *Molecular Microbiology*. 2005; 55:637–652. doi: [10.1111/j.1365-2958.2004.04414.x](#) PMID: [15659176](#)
24. Palige K, Linde J, Martin R, Bottcher B, Citiulo F, Sullivan DJ, et al. Global transcriptome sequencing identifies chlamyospore specific markers in *Candida albicans* and *Candida dubliniensis*. *PLoS One*. 2013; 8:e61940. doi: [10.1371/journal.pone.0061940](#) PMID: [23613980](#)
25. Cole GT, Seshan KR, Phaneuf M, Lynn KT. Chlamyospore-like cells of *Candida albicans* in the gastrointestinal tract of infected, immunocompromised mice. *Can J Microbiol*. 1991; 37:637–646. PMID: [1954577](#)
26. Heineman HS, Yunis EJ, Siemienski J, Braude AI. Chlamyospores and dimorphism in *Candida albicans* endocarditis. Observations in a fatal superinfection during treatment of staphylococcus endocarditis. *Arch Intern Med*. 1961; 108:570–577. PMID: [14042292](#)
27. Ho PC, O'Day DM. Candida endophthalmitis and infection of costal cartilages. *Br J Ophthalmol*. 1981; 65:333–334. doi: [10.1136/bjo.65.5.333](#) PMID: [6972782](#)
28. Navarathna DH, Hornby JM, Hoerrmann N, Parkhurst AM, Duhamel GE, Nickerson KW. Enhanced pathogenicity of *Candida albicans* pre-treated with subinhibitory concentrations of fluconazole in a mouse model of disseminated candidiasis. *J Antimicrob Chemother*. 2005; 56:1156–1159. doi: [10.1093/jac/dki383](#) PMID: [16239285](#)
29. Dumitru R, Navarathna DH, Semighini CP, Elowsky CG, Dumitru RV, Dignard D, et al. In vivo and in vitro anaerobic mating in *Candida albicans*. *Eukaryot Cell*. 2007; 6:465–472. doi: [10.1128/EC.00316-06](#) PMID: [17259544](#)
30. Navarathna DH, Hornby JM, Krishnan N, Parkhurst A, Duhamel GE, Nickerson KW. Effect of farnesol on a mouse model of systemic candidiasis, determined by use of a DPP3 knockout mutant of *Candida albicans*. *Infect Immun*. 2007; 75:1609–1618. doi: [10.1128/IAI.01182-06](#) PMID: [17283095](#)
31. Navarathna DH, Nickerson KW, Duhamel GE, Jerrels TR, Petro TM. Exogenous farnesol interferes with the normal progression of cytokine expression during candidiasis in a mouse model. *Infect Immun*. 2007; 75:4006–4011. doi: [10.1128/IAI.00397-07](#) PMID: [17517874](#)
32. Kebaara BW, Langford ML, Navarathna DH, Dumitru R, Nickerson KW, Atkin AL. *Candida albicans* Tup1 is involved in farnesol-mediated inhibition of filamentous-growth induction. *Eukaryot Cell*. 2008; 7:980–987. doi: [10.1128/EC.00357-07](#) PMID: [18424510](#)
33. Ghosh S, Navarathna DH, Roberts DD, Cooper JT, Atkin AL, Petro TM, et al. Arginine-induced germ tube formation in *Candida albicans* is essential for escape from murine macrophage line RAW 264.7. *Infect Immun*. 2009; 77:1596–1605. doi: [10.1128/IAI.01452-08](#) PMID: [19188358](#)
34. Navarathna DH, Roberts DD. *Candida albicans* heme oxygenase and its product CO contribute to pathogenesis of candidemia and alter systemic chemokine and cytokine expression. *Free Radic Biol Med*. 2010; 49:1561–1573. doi: [10.1016/j.freeradbiomed.2010.08.020](#) PMID: [20800092](#)
35. Navarathna DH, Das A, Morschhauser J, Nickerson KW, Roberts DD. Dur3 is the major urea transporter in *Candida albicans* and is co-regulated with the urea amidolyase Dur1,2. *Microbiology*. 2011; 157:270–279. doi: [10.1099/mic.0.045005-0](#) PMID: [20884691](#)
36. Martin-Manso G, Navarathna DH, Galli S, Soto-Pantoja DR, Kuznetsova SA, Tsokos M, et al. Endogenous thrombospondin-1 regulates leukocyte recruitment and activation and accelerates death from systemic candidiasis. *PLoS One*. 2012; 7:e48775. doi: [10.1371/journal.pone.0048775](#) PMID: [23144964](#)
37. Navarathna DH, Lionakis MS, Lizak MJ, Munasinghe J, Nickerson KW, Roberts DD. Urea amidolyase (DUR1,2) contributes to virulence and kidney pathogenesis of *Candida albicans*. *PLoS One*. 2012; 7:e48475. doi: [10.1371/journal.pone.0048475](#) PMID: [23144764](#)

38. Navarathna DH, Munasinghe J, Lizak MJ, Nayak D, McGavern DB, Roberts DD. MRI confirms loss of blood-brain barrier integrity in a mouse model of disseminated candidiasis. *NMR Biomed.* 2013; 26:1125–1134. doi: [10.1002/nbm.2926](https://doi.org/10.1002/nbm.2926) PMID: [23606437](https://pubmed.ncbi.nlm.nih.gov/23606437/)
39. Fazio TG, Kooperberg C, Goldmark JP, Neal C, Basom R, Delrow J, et al. Widespread collaboration of Isw2 and Sin3-Rpd3 chromatin remodeling complexes in transcriptional repression. *Mol Cell Biol.* 2001; 21:6450–6460. doi: [10.1128/MCB.21.19.6450-6460.2001](https://doi.org/10.1128/MCB.21.19.6450-6460.2001) PMID: [11533234](https://pubmed.ncbi.nlm.nih.gov/11533234/)
40. Goldmark JP, Fazio TG, Estep PW, Church GM, Tsukiyama T. The Isw2 chromatin remodeling complex represses early meiotic genes upon recruitment by Ume6p. *Cell.* 2000; 103:423–433. doi: [10.1016/S0092-8674\(00\)00134-3](https://doi.org/10.1016/S0092-8674(00)00134-3) PMID: [11081629](https://pubmed.ncbi.nlm.nih.gov/11081629/)
41. Riedel CG, Downen RH, Lourenco GF, Kirienco NV, Heimbucher T, West JA, et al. DAF-16 employs the chromatin remodeller SWI/SNF to promote stress resistance and longevity. *Nat Cell Biol.* 2013; 15:491–501. doi: [10.1038/ncb2720](https://doi.org/10.1038/ncb2720) PMID: [23604319](https://pubmed.ncbi.nlm.nih.gov/23604319/)
42. Trachtulcova P, Janatova I, Kohlwein SD, Hasek J. *Saccharomyces cerevisiae* gene *ISW2* encodes a microtubule-interacting protein required for premeiotic DNA replication. *Yeast.* 2000; 16:35–47. doi: [10.1002/\(sici\)1097-0061\(20000115\)16:1<35::aid-yea504>3.0.co;2-0](https://doi.org/10.1002/(sici)1097-0061(20000115)16:1<35::aid-yea504>3.0.co;2-0) PMID: [10620773](https://pubmed.ncbi.nlm.nih.gov/10620773/)
43. Tsukiyama T, Palmer J, Landel CC, Shiloach J, Wu C. Characterization of the imitation switch subfamily of ATP-dependent chromatin-remodeling factors in *Saccharomyces cerevisiae*. *Genes Dev.* 1999; 13:686–697. doi: [10.1101/gad.13.6.686](https://doi.org/10.1101/gad.13.6.686) PMID: [10090725](https://pubmed.ncbi.nlm.nih.gov/10090725/)
44. Gillum AM, Tsay EY, Kirsch DR. Isolation of the *Candida albicans* gene for orotidine-5'-phosphate decarboxylase by complementation of *S. cerevisiae* *ura3* and *E. coli* *pyrF* mutations. *Mol Gen Genet.* 1984; 198:179–182. doi: [10.1007/BF00328721](https://doi.org/10.1007/BF00328721) PMID: [6394964](https://pubmed.ncbi.nlm.nih.gov/6394964/)
45. Cannon RD, Niimi K, Jenkinson HF, Shepherd MG. Molecular cloning and expression of the *Candida albicans* beta-N-acetylglucosaminidase (HEX1) gene. *J Bacteriol.* 1994; 176:2640–2647. PMID: [8169213](https://pubmed.ncbi.nlm.nih.gov/8169213/)
46. Nakamoto S. Germ tube formation of *Candida albicans* in corn meal broth using the non-slip slide glass incubation method. *Yonago Acta medica.* 1998; 41:65–72.
47. Staib P, Morschhauser J. Chlamyospore formation on Staib agar as a species-specific characteristic of *Candida dubliniensis*. *Mycoses.* 1999; 42:521–524. doi: [10.1046/j.1439-0507.1999.00516.x](https://doi.org/10.1046/j.1439-0507.1999.00516.x) PMID: [10592694](https://pubmed.ncbi.nlm.nih.gov/10592694/)
48. Brakke MK. Density Gradient Centrifugation: A New Separation Technique. *J Am Chem Soc.* 1951; 73:1847–1848. doi: [10.1021/ja01148a508](https://doi.org/10.1021/ja01148a508)
49. Reuss O, Vik A, Kolter R, Morschhauser J. The SAT1 flipper, an optimized tool for gene disruption in *Candida albicans*. *Gene.* 2004; 341:119–127. doi: [10.1016/j.gene.2004.06.021](https://doi.org/10.1016/j.gene.2004.06.021) PMID: [15474295](https://pubmed.ncbi.nlm.nih.gov/15474295/)
50. Sasse C, Morschhauser J. Gene deletion in *Candida albicans* wild-type strains using the SAT1-flipping strategy. *Methods Mol Biol.* 2012; 845:3–17. doi: [10.1007/978-1-61779-539-8_1](https://doi.org/10.1007/978-1-61779-539-8_1) PMID: [22328364](https://pubmed.ncbi.nlm.nih.gov/22328364/)
51. Hornby JM, Dumitru R, Nickerson KW. High phosphate (up to 600 mM) induces pseudohyphal development in five wild type *Candida albicans*. *J Microbiol Methods.* 2004; 56:119–124. doi: [10.1016/j.mimet.2003.09.021](https://doi.org/10.1016/j.mimet.2003.09.021) PMID: [14706756](https://pubmed.ncbi.nlm.nih.gov/14706756/)
52. Zhang H, Siede W. Analysis of the budding yeast *Saccharomyces cerevisiae* cell cycle by morphological criteria and flow cytometry. *Methods Mol Biol.* 2004; 241:77–91. doi: [10.1385/1-59259-646-0:77](https://doi.org/10.1385/1-59259-646-0:77) PMID: [14970647](https://pubmed.ncbi.nlm.nih.gov/14970647/)
53. Barelle CJ, Bohula EA, Kron SJ, Wessels D, Soll DR, Schäfer A, et al. Asynchronous cell cycle and asymmetric vacuolar inheritance in true hyphae of *Candida albicans*. *Eukaryotic Cell.* 2003; 2:398–410. doi: [10.1128/EC.2.3.398-410.2003](https://doi.org/10.1128/EC.2.3.398-410.2003) PMID: [12796285](https://pubmed.ncbi.nlm.nih.gov/12796285/)
54. Kohrer K, Domdey H. Preparation of high molecular weight RNA. *Methods Enzymol.* 1991; 194:398–405. doi: [10.1016/0076-6879\(91\)94030-G](https://doi.org/10.1016/0076-6879(91)94030-G) PMID: [1706459](https://pubmed.ncbi.nlm.nih.gov/1706459/)
55. Pendrak ML, Yan SS, Roberts DD. Hemoglobin regulates expression of an activator of mating-type locus alpha genes in *Candida albicans*. *Eukaryot Cell.* 2004; 3:764–775. doi: [10.1128/ec.3.3.764-775.2004](https://doi.org/10.1128/ec.3.3.764-775.2004) PMID: [15189997](https://pubmed.ncbi.nlm.nih.gov/15189997/)
56. Louria DB, Brayton RG, Finkel G. Studies on the pathogenesis of experimental *Candida albicans* infections in mice. *Med Mycol.* 1963; 2:271–283. doi: [10.1080/00362176385190431](https://doi.org/10.1080/00362176385190431)
57. MacCallum DM, Odds FC. Temporal events in the intravenous challenge model for experimental *Candida albicans* infections in female mice. *Mycoses.* 2005; 48:151–161. doi: [10.1111/j.1439-0507.2005.01121.x](https://doi.org/10.1111/j.1439-0507.2005.01121.x) PMID: [15842329](https://pubmed.ncbi.nlm.nih.gov/15842329/)
58. Lionakis MS, Lim JK, Lee CC, Murphy PM. Organ-specific innate immune responses in a mouse model of invasive candidiasis. *J Innate Immun.* 2011; 3:180–199. doi: [10.1159/000321157](https://doi.org/10.1159/000321157) PMID: [21063074](https://pubmed.ncbi.nlm.nih.gov/21063074/)
59. Jansons VK, Nickerson WJ. Chemical composition of chlamyospores of *Candida albicans*. *J Bacteriol.* 1970; 104:922–932. PMID: [4099099](https://pubmed.ncbi.nlm.nih.gov/4099099/)

60. Chibana H, Uno J, Cho T, Mikami Y. Mutation in IRO1 tightly linked with URA3 gene reduces virulence of *Candida albicans*. *Microbiol Immunol*. 2005; 49:937–939. PMID: [16237272](#)
61. Kirsch DR, Whitney RR. Pathogenicity of *Candida albicans* auxotrophic mutants in experimental infections. *Infect Immun*. 1991; 59:3297–3300. PMID: [1879944](#)
62. Lay J, Henry LK, Clifford J, Koltin Y, Bulawa CE, Becker JM. Altered expression of selectable marker URA3 in gene-disrupted *Candida albicans* strains complicates interpretation of virulence studies. *Infect Immun*. 1998; 66:5301–5306. PMID: [9784536](#)
63. Cheng S, Nguyen MH, Zhang Z, Jia H, Handfield M, Clancy CJ. Evaluation of the Roles of Four *Candida albicans* Genes in Virulence by Using Gene Disruption Strains That Express URA3 from the Native Locus. *Infection and Immunity*. 2003; 71:6101–6103. doi: [10.1128/iai.71.10.6101-6103.2003](#) PMID: [14500538](#)
64. Palmer GE, Johnson KJ, Ghosh S, Sturtevant J. Mutant alleles of the essential 14-3-3 gene in *Candida albicans* distinguish between growth and filamentation. *Microbiology*. 2004; 150:1911–1924. doi: [10.1099/mic.0.26910-0](#) PMID: [15184577](#)
65. Palmer GE, Sturtevant JE. Random mutagenesis of an essential *Candida albicans* gene. *Curr Genet*. 2004; 46:343–356. doi: [10.1007/s00294-004-0538-0](#) PMID: [15549319](#)
66. Al-Hedaithy SS, Fotedar R. Recovery and studies on chlamyospore-negative *Candida albicans* isolated from clinical specimens. *Med Mycol*. 2002; 40:301–306. doi: [10.1080/714031115](#) PMID: [12146760](#)
67. Alasio TM, Lento PA, Bottone EJ. Giant blastoconidia of *Candida albicans*. A case report and review of the literature. *Arch Pathol Lab Med*. 2003; 127:868–871. doi: [10.1043/1543-2165\(2003\)127<868:GBOCA>2.0.CO;2](#) PMID: [12823045](#)
68. Bottone EJ, Horga M, Abrams J. "Giant" blastoconidia of *Candida albicans*: morphologic presentation and concepts regarding their production. *Diagn Microbiol Infect Dis*. 1999; 34:27–32. doi: [10.1016/S0732-8893\(99\)00013-9](#) PMID: [10342104](#)
69. Chabasse D, Bouchara JP, de Gentile L, Chennebault JM. *Candida albicans* chlamyospores observed in vivo in a patient with AIDS. *Ann Biol Clin (Paris)*. 1988; 46:817–818. PMID: [3069016](#)
70. Schonborn C, Schmidt G. Demonstration of *Candida albicans* chlamyospores in the dermatological specimen. *Mykosen*. 1971; 14:119–125. PMID: [4926906](#)
71. Wilborn WH, Montes LF. Scanning electron microscopy of oral lesions in chronic mucocutaneous candidiasis. *JAMA*. 1980; 244:2294–2297. doi: [10.1001/jama.1980.03310200034022](#) PMID: [7001057](#)
72. Caretta G, Del Frate G, Guglielminetti M. Evaluation of the antigen from chlamyospores of *Candida albicans* in the serodiagnosis of candidiasis. *Mycopathologia*. 1982; 77:159–163. doi: [10.1007/BF00518801](#) PMID: [6803168](#)
73. Sullivan DJ, Westerneng TJ, Haynes KA, Bennett DE, Coleman DC. *Candida dubliniensis* sp. nov.: phenotypic and molecular characterization of a novel species associated with oral candidosis in HIV-infected individuals. *Microbiology*. 1995; 141 (Pt 7):1507–1521. doi: [10.1099/13500872-141-7-1507](#) PMID: [7551019](#)
74. Irving SG, Zipfel PF, Balke J, McBride OW, Morton CC, Burd PR, et al. Two inflammatory mediator cytokine genes are closely linked and variably amplified on chromosome 17q. *Nucleic Acids Res*. 1990; 18:3261–3270. doi: [10.1093/nar/18.11.3261](#) PMID: [1972563](#)
75. Lionakis MS. New insights into innate immune control of systemic candidiasis. *Med Mycol*. 2014; 52:555–564. doi: [10.1093/mmy/myu029](#) PMID: [25023483](#)
76. Dang W, Sutphin GL, Dorsey JA, Otte GL, Cao K, Perry RM, et al. Inactivation of yeast Isw2 chromatin remodeling enzyme mimics longevity effect of calorie restriction via induction of genotoxic stress response. *Cell Metab*. 2014; 19:952–966. doi: [10.1016/j.cmet.2014.04.004](#) PMID: [24814484](#)
77. Kaerberlein M, Powers RW, Steffen KK, Westman EA, Hu D, Dang N, et al. Regulation of Yeast Replicative Life Span by TOR and Sch9 in Response to Nutrients. *Science*. 2005; 310:1193–1196. doi: [10.1126/science.1115535](#) PMID: [16293764](#)
78. Daróczy J, Galgóczy J, Simon G. Scanning electron microscopy of *Candida albicans* chlamyospores. *Mycoses*. 1988; 31:523–526. doi: [10.1111/j.1439-0507.1988.tb04404.x](#) PMID: [3063963](#)
79. Bakerspigel A, Burke S. A possible function of the chlamyospores of *Candida albicans*. *Mycopathol Mycol Appl*. 1974; 54:147–152. PMID: [4610380](#)
80. Wilson RB, Davis D, Mitchell AP. Rapid Hypothesis Testing with *Candida albicans* through Gene Disruption with Short Homology Regions. *Journal of Bacteriology*. 1999; 181:1868–1874. PMID: [10074081](#)